EXPERIMENTAL DETERMINATION OF THE ULTIMATE CAPACITY OF A COMPOSITE PRESTRESSED BRIDGE UNIT

FINAL REPORT

by

RAJENDRA PRASAD
Research Assistant
and
BENJAMIN WALLACE
and
THOMAS D. BUSH JR.
Co-Principal Investigators

DECEMBER 1989

sponsored by

OKLAHOMA DEPARTMENT OF TRANSPORTATION
RESEARCH AND DEVELOPMENT DIVISION
in cooperation with the
FEDERAL HIGHWAY ADMINISTRATION

conducted at

FEARS STRUCTURAL ENGINEERING LABORATORY
SCHOOL OF CIVIL ENGINEERING AND ENVIRONMENTAL SCIENCE
UNIVERSITY OF OKLAHOMA, NORMAN, OKLAHOMA

TECHNICAL REPORT STANDARD TITLE PAGE

1. REPORT NO. FHWA/OK 89(05)	2. GOVERNMENT ACCESSION NO.	3. RECIPIENT'S CATALOG NO.
4. TITLE AND SUBTITLE Experimental Determination of the Ultimate Capacity of a Composite Prestressed Bridge Unit		5. REPORT DATE December 1989
		6. PERFORMING ORGANIZATION CODE
7. AUTHOR(S) Rajendra Prasad, Benjamin Wallace, and Thomas D. Bush Jr.		8. PERFORMING ORGANIZATION REPORT
9. PERFORMING ORGANIZATION AND ADDRESS Fears Structural Engineering Laboratory University of Oklahoma 303 E. Chesapeake, Norman, OK 73019		10. WORK UNIT NO.
		11. CONTRACT OR GRANT NO. Agreement No. 2162
12. SPONSORING AGENCY NAME AND ADDRESS Research and Development Division Oklahoma Department of Transportation 200 NE 21st Oklahoma City, OK 73105		13. TYPE OF REPORT AND PERIOD COVERED Final
		14. SPONSORING AGENCY CODE

15. SUPPLEMENTARY NOTES in cooperation with
Federal Highway Administration, US Department of Transportation

16. ABSTRACT

A 55 ft. long prestressed, composite steel girder-concrete slab bridge unit was tested to ultimate load. The unit had previously undergone a series of tests including sustained loading, fatigue loading, and static loading to first yield.

The 54 ft., simply supported span was subjected to static loads applied at points 20 ft. from the supports. Vertical deflection as measured at midspan, and horizontal slippage at the slab-girder interface was measured at several locations along the span. Strain gage readings at midspan throughout the depth of the unit were recorded.

The bridge unit behaved in a ductile manner, deflecting 18.6 inches before failure occurred. Failure was by crushing of the slab at the load application points. The unit supported an applied load 13% greater than the ultimate load predicted. The excess capacity is attributed to strain hardening of the bottom flanges of the girders. Slippage at the slab-girder interface was observed to be small. Existing analysis procedures were found to be adequate for predicting the ultimate capacity of the unit.

Load at first yield in a previous test was observed to be lower than predicted. It was determined that the reduction in yield load can be explained by the presence of residual tensile rolling stresses in the bottom flanges of the girders.

17. KEY WORDS bridge, prestressed, composite, pre-fabricated	18. DISTRIBUTION STATEMENT No Restrictions

19. SECURITY CLASSIF. (OF THIS REPORT) None	20. SECURITY CLASSIF. (OF THIS PAGE)	21. NO. OF PAGES	22. PRICE

METRIC (SI*) CONVERSION FACTORS

APPROXIMATE CONVERSIONS TO SI UNITS

Symbol	When You Know	Multiply By	To Find	Symbol
		LENGTH		
in	inches	2.54	millimetres	mm
ft	feet	0.3048	metres	m
yd	yards	0.914	metres	m
mi	miles	1.61	kilometres	km
		AREA		
in^2	square inches	645.2	millimetres squared	mm^2
ft^2	square feet	0.0929	metres squared	m^2
yd^2	square yards	0.836	metres squared	m^2
mi^2	square miles	2.59	kilometres squared	km^2
ac	acres	0.395	hectares	ha
		MASS (weight)		
oz	ounces	28.35	grams	g
lb	pounds	0.454	kilograms	kg
T	short tons (2000 lb)	0.907	megagrams	Mg
		VOLUME		
fl oz	fluid ounces	29.57	millilitres	mL
gal	gallons	3.785	litres	L
ft^3	cubic feet	0.0328	metres cubed	m^3
yd^3	cubic yards	0.0765	metres cubed	m^3

NOTE: Volumes greater than 1000 L shall be shown in m^3.

		TEMPERATURE (exact)		
°F	Fahrenheit temperature	5/9 (after subtracting 32)	Celsius temperature	°C

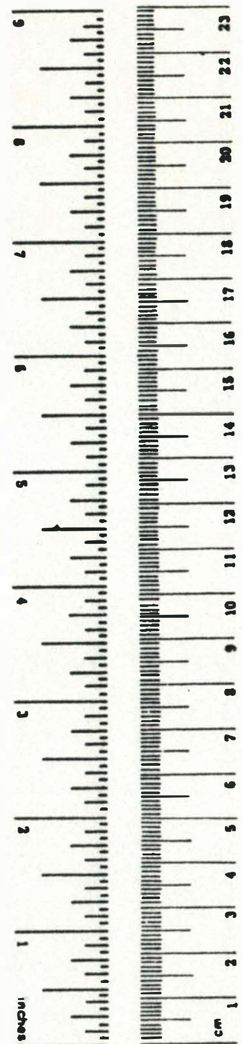

APPROXIMATE CONVERSIONS TO SI UNITS

Symbol	When You Know	Multiply By	To Find	Symbol
		LENGTH		
mm	millimetres	0.039	inches	in
m	metres	3.28	feet	ft
m	metres	1.09	yards	yd
km	kilometres	0.621	miles	mi
		AREA		
mm^2	millimetres squared	0.0016	square inches	in^2
m^2	metres squared	10.764	square feet	ft^2
km^2	kilometres squared	0.39	square miles	mi^2
ha	hectores (10 000 m^2)	2.53	acres	ac
		MASS (weight)		
g	grams	0.0353	ounces	oz
kg	kilograms	2.205	pounds	lb
Mg	megagrams (1 000 kg)	1.103	short tons	T
		VOLUME		
mL	millilitres	0.034	fluid ounces	fl oz
L	litres	0.264	gallons	gal
m^3	metres cubed	35.315	cubic feet	ft^3
m^3	metres cubed	1.308	cubic yards	yd^3

		TEMPERATURE (exact)		
°C	Celsius temperature	9/5 (then add 32)	Fahrenheit temperature	°F

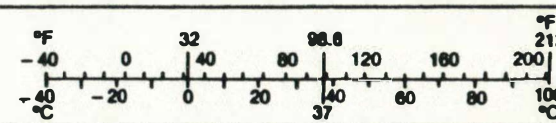

These factors conform to the requirement of FHWA Order 5190.1A.

* SI is the symbol for the International System of Measurements

ABSTRACT

A 55 ft. long prestressed, composite steel girder-concrete slab bridge unit was tested to ultimate load. The unit had previously undergone a series of tests including sustained loading, fatigue loading, and static loading to first yield.

The 54 ft., simply supported span was subjected to static loads applied over the girders at points 20 ft. from the supports. Vertical deflections were measured at the supports and midspan, and horizontal slippage at the slab-girder interface was measured at several locations along the span. Strain gage readings at midspan on the slab surface, slab longitudinal bars, and throughout the depth of the girders were recorded.

The bridge unit behaved in a ductile manner, deflecting 18.6 inches before failure occurred. Strain gage readings indicated yielding occurred over nearly the full depth of the girders. Failure was by crushing of the slab at the load application points. The unit supported an applied load 13% greater than the ultimate load predicted using actual material properties. The excess capacity is attributed to strain hardening of the bottom flanges of the girders. Slippage at the slab-girder interface was observed to be small. Existing analysis procedures were found to be adequate for predicting the ultimate capacity of the unit.

Load at first yield in a previous test was observed to be lower than predicted. It was determined that the reduction in yield load can be explained by the presence of residual tensile rolling stresses in the bottom flanges of the girders.

TABLE OF CONTENTS

LIST OF FIGURES

LIST OF TABLES

EXPERIMENTAL DETERMINATION OF THE ULTIMATE CAPACITY OF A COMPOSITE PRESTRESSED BRIDGE UNIT

CHAPTER I

INTRODUCTION

1.1 General

This report documents the ultimate load capacity test of a full size composite prestressed bridge unit. Previous research conducted at the Fears Structural Engineering Laboratory, University of Oklahoma, studied the effects of sustained, fatigue, and static loading on these units [1,2].

The prestressed composite bridge unit studied was manufactured from two steel girders attached to a concrete slab with shear connectors as shown in Figure 1.1. These units are prefabricated and transported to a site, where they are placed on abutments. The units are then connected to each other with steel angle x-brace diaphragms. Guard rails are attached to complete the bridge.

The method used to produce the units is unique and patented. This method outlined below is described in detail in the previous research reports [1, 2]. First, shear connectors are welded to the steel girders which are then inverted and simply supported. Next a re-usable slab form is suspended from the girders as shown in Figure 1.2. Reinforcing bars and concrete are placed in the form and additional load is applied to the steel girders if required to obtain the desired inverse deflection. After the concrete has hardened, the form is removed and the unit is turned upright. The resulting composite unit has locked-in stresses due to the

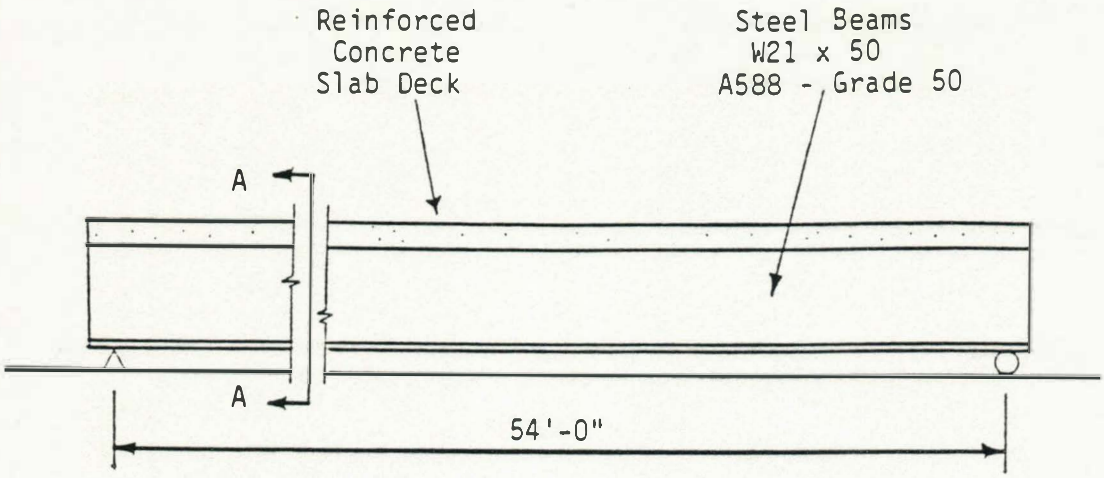

(a) Elevation

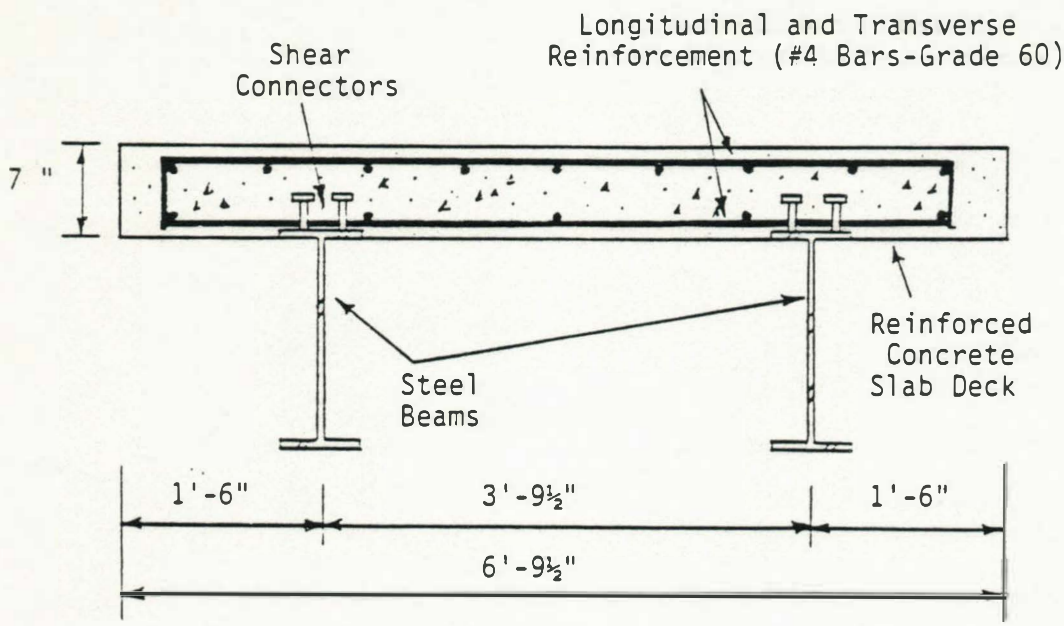

(b) Section A-A

Figure 1.1 Typical Bridge Unit Configuration
(Reference 2)

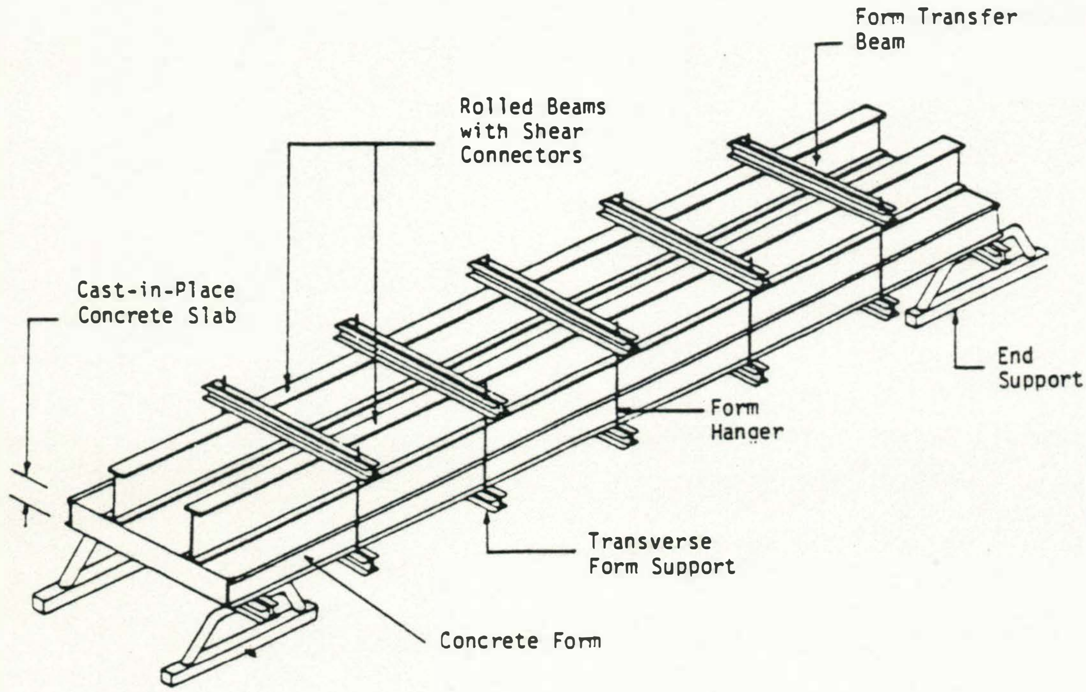

Figure 1.2 Method of Bridge Unit Fabrication

(Reference 2)

reverse curvature imposed on the girders before the concrete hardened. This was the only means of prestressing used on the unit tested.

The resulting prestressing extends the service load range as indicated in Figure 1.3. The prestressing has no effect on the ultimate moment capacity as the ductile steel girders can yield until a plastic moment capacity is achieved. The plastic moment capacity is not affected by locked-in internal stresses.

Another possible advantage of this type of construction is reduced water permeability of the deck top surface. The inverted position when the deck is cast results in bleedwater migrating to the girder side of the deck, leaving the least permeable concrete next to the form. Thus, the least permeable concrete ends up on the top surface of the bridge slab. This advantageous positioning of the least permeable concrete may reduce reinforcing bar corrosion problems and accompanying maintenance problems.

Two of these bridge units had been tested previously. Details of these specimens and the testing conducted previously can be found in the previous research reports [1, 2]. Related portions of the previous reports are summarized here to give a full history of the specimen tested in this research project. The previous research program studied the effects of long-term sustained loading, repeated (fatigue) loading, and static loading. The static loading test of the first bridge unit was terminated when repairs to fatigue cracks failed, rendering the test of ultimate capacity inconclusive. The static loading test of the second bridge unit was terminated shortly after yielding was observed to preserve the unit for possible re-use. Testing of the second bridge unit was continued in this study.

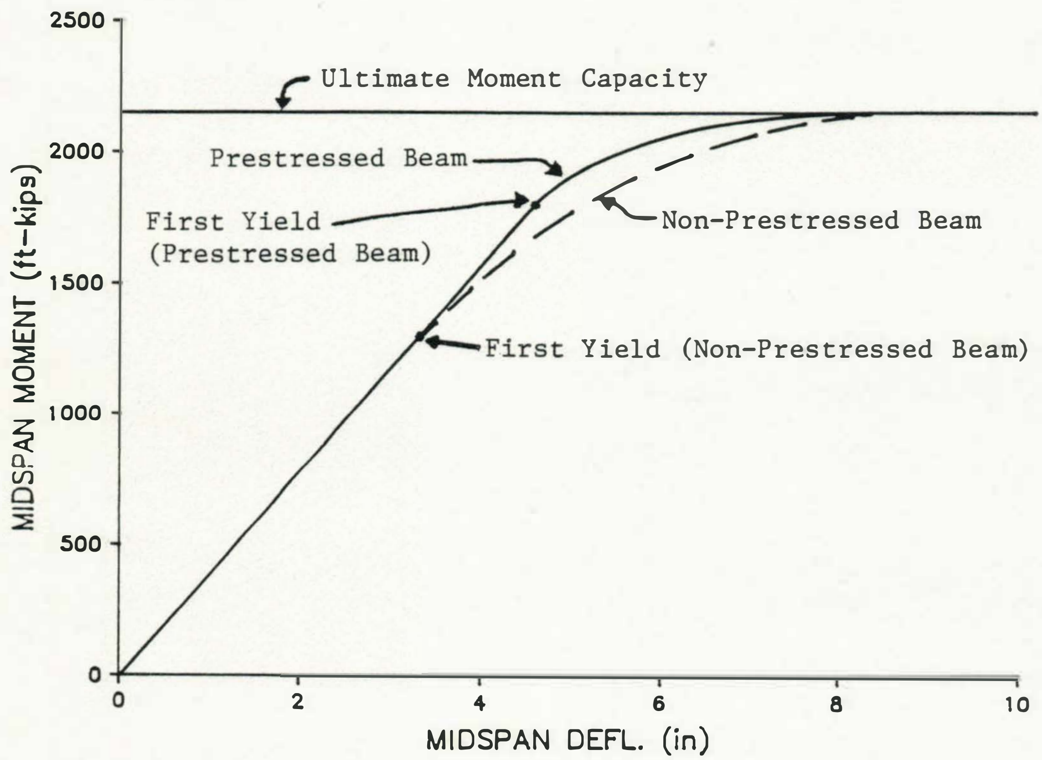

Figure 1.3 Bridge Unit Moment vs. Midspan Deflection

1.2 Objectives

The objectives of this research project are:

a) To experimentally determine the ultimate capacity of the composite prestressed bridge unit. This test was desired as all previous tests of these units were stopped before the predicted ultimate capacity was reached.

b) To investigate the apparent early yielding of these bridge units observed in previous tests. The causes of this early yielding were not fully reported previously.

c) To investigate the relationship between load and horizontal slip at the slab-girder interface. This topic is of interest to ensure that the shear connector design was adequate.

1.3 Scope

The scope of this research project was to continue testing of the second bridge unit studied in the previous research project. The loading apparatus used in the previous static load tests was re-used. The loading program was limited to a single static load applied until failure occurred. Data collected included load, vertical deflection, strains at various locations at midspan, and horizontal slip between the steel girders and the concrete slab at various sections.

CHAPTER II

PREVIOUS RESEARCH ON COMPOSITE PRESTRESSED BRIDGE UNIT

2.1 Test Specimen Description

The second bridge unit tested previously consisted of two W21x50 steel girders, 3x3x1/4 in. steel angle cross-frame diaphragms, and a 7 in. thick concrete slab [1, 2] as shown previously in Figure 1.1. The units were 55 ft. long and had slabs 6 ft. - 9 1/2 in. wide. Cross-frame diaphragms were located at each end and at third span intervals. Pairs of 3/4 in. diameter by 4 in. high shear studs were welded to the top flange of each girder in accordance with the AASHTO specification [3]. The resulting stud layout is shown in Figure 2.1. Two layers of number 4 grade 60 reinforcing bars were placed in the slabs as indicated in Figure 2.2. The slabs were cast using 5000 psi design strength concrete. Material properties measured for each specimen are given in Table 2.1.

2.2 Test Procedure and Results

Results of both bridge tests are reported in References 1 and 2. The second bridge unit was subjected to fatigue, sustained loading, and static loading tests. The loading history of the second bridge, which should be kept in mind when evaluating the static test results, is as follows: The unit was cast on March 19, 1986 and brought into FSEL on April 18, 1986. During the period from April 22, 1986 to May 22, 1986, the bridge unit was subjected to 500,000 cycles of HS-20 loading. On May 28, 1986 a static test was performed on the unit, with the loading stopped when the calculated first yield moment was applied. The unit was then

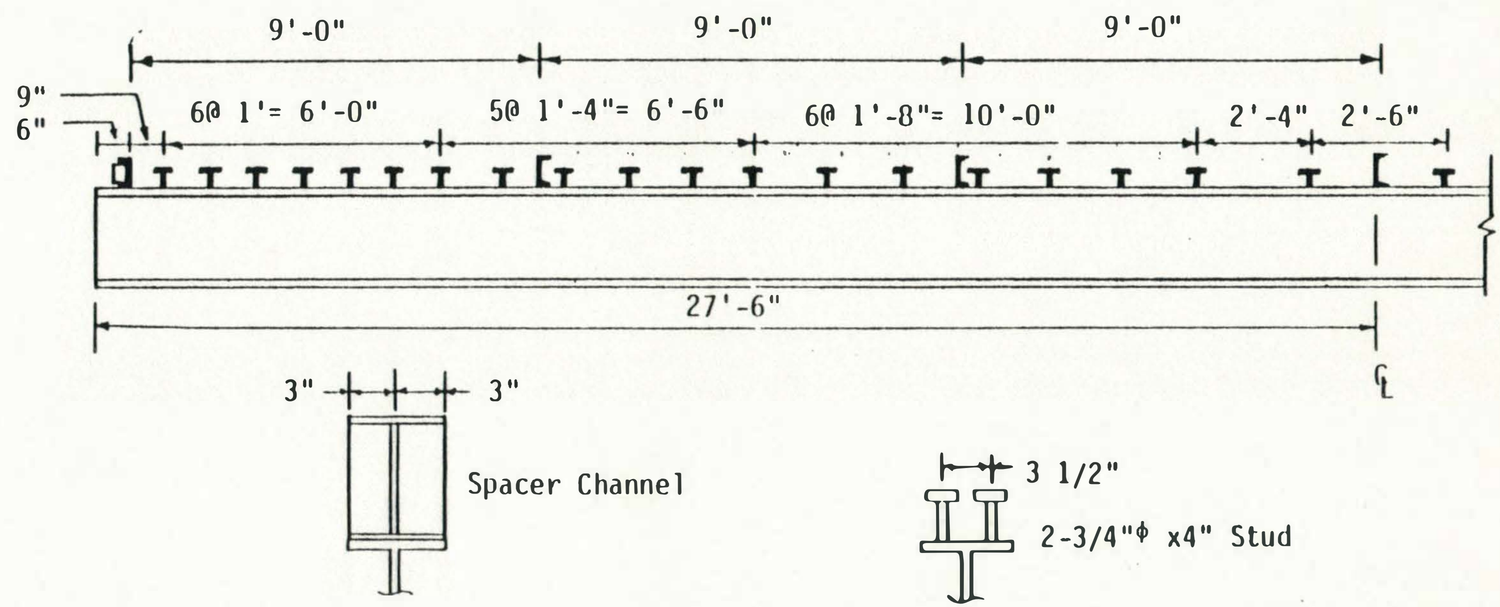

Figure 2.1 Bridge Unit Shear Connector Layout

(Reference 2)

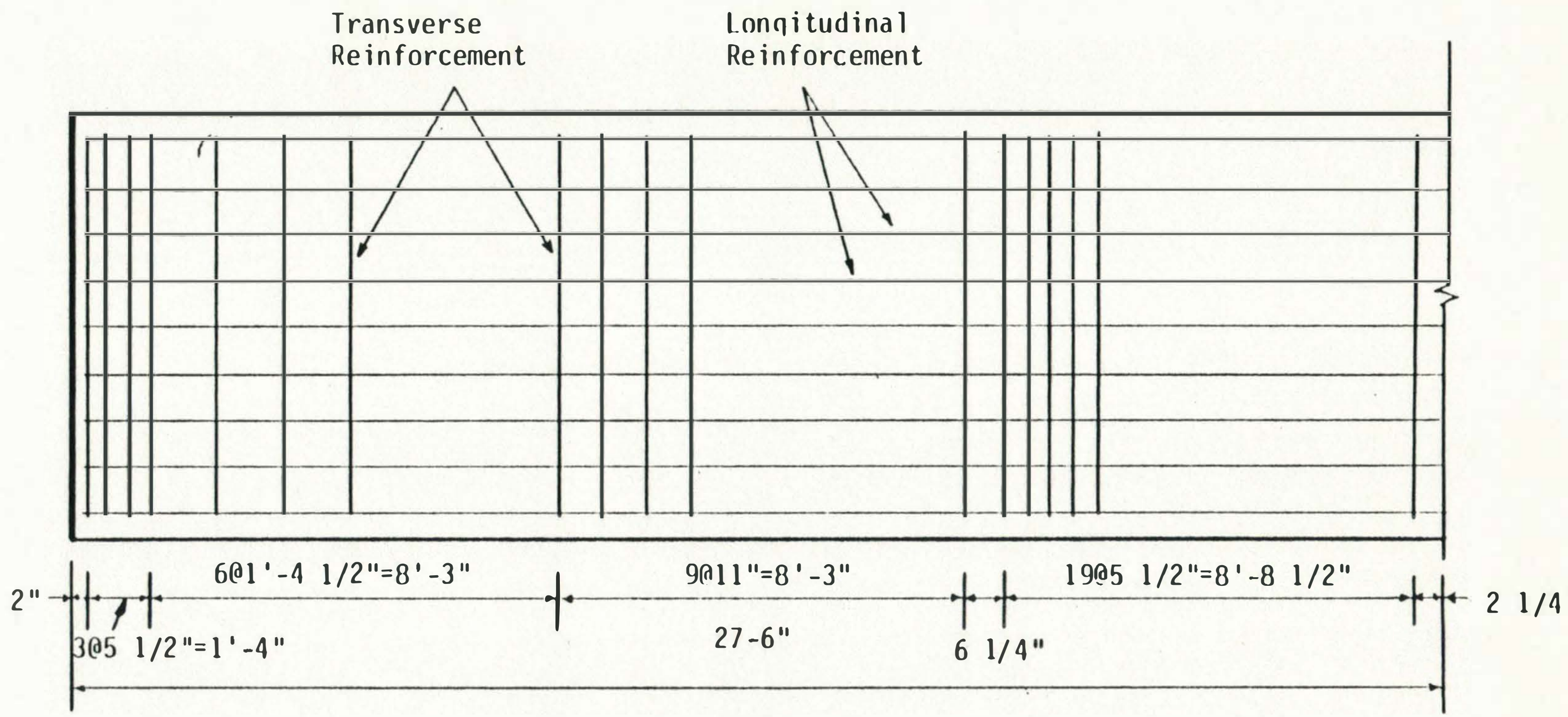

Figure 2.2 Bridge Unit Slab Reinforcement Layout
(Reference 2)

Table 2.1
Material Properties
(From Reference 1)

(a) Steel girders (W21x50, A588 Grade 50 Steel)

Test Specimen	Yield Stress (ksi)	Elastic Modulus (ksi)
First Unit	56.0	29000. *
Second Unit	58.0	29000. *

(b) Reinforcement (#4 Bar - Grade 60)

Test Specimen	Yield Stress (ksi)	Elastic Modulus (ksi)
First Unit	67.2	29000. *
Second Unit	-	29000. *
Control Slabs	79.5	-
Shear Connector Specimens	-	-

(c) Concrete (5.0 ksi Design Strength)

Test Specimen	Age at Cylinder Test (days)	Compressive Strength (ksi)	Elastic Modulus (ksi)
First Unit	28	5.30	4394. *
	1408	7.40	4365.
Second Unit	51	6.45	5335.
Control Slabs	120	6.54	-
Shear Connector Specimens	28	5.74	-

* Assumed
\- Not Required

removed from the Laboratory and subjected to a sustained dead load from June 3, 1986 until July, 1988. Only details from the previous static load test are reviewed here for comparison with the results of this study. The test setup was essentially the same as used in this study and described in Chapter 3.

Strain gages installed at the midspan of the steel girders of bridge unit #2 were connected to an indicator during fabrication. These strains along with camber measurements were recorded at key steps in the manufacturing process to verify the expected prestressing strains. The resulting values and increments from one manufacturing step to the next are given in Table 2.2. A discussion of the predicted stresses listed in Table 2.2 is given in Appendix B.

The bridge unit was simply supported on neoprene bearing pads and cribbing at each end for a span of 54 feet. Two transverse and one longitudinal spreader girders were used to distribute the applied load to two points fourteen feet apart centered over each steel girder. The load was applied by a hydraulic ram and measured with an electronic load cell. The weight of the spreader girders was then added to the load cell reading to obtain the values reported as "Load." Vertical displacements were measured at the midspan and both ends of each girder with linear potentiometers and Linear Variable Displacement Transformers (LVDTs), respectively. Horizontal slip between the concrete slab and the upper flange of each girder was measured using dial gages at seven locations along the length of each girder.

The resulting load vs. deflection diagram from the prior static load test is shown in Figure 2.3. It should be noted that the load shown in this figure includes the 7.0 kip weight of the spreader girder assembly. In addition to the curve indicating the experimental results, this figure includes a sloping dashed line which represents the theoretical elastic behavior and three horizontal lines which represent calculated capacities.

Table 2.2
Changes in Bottom Flange Stress and Camber
(from Reference 1)

Loading Step	Measured Bottom Flange Stress (ksi)	Change in Measured Bottom Flange Stress (ksi)	Predicted Bottom Flange Stress (ksi)	Change in Predicted Bottom Flange Stress (ksi)	Measured Camber (in)	Change in Measured Camber (in)	Predicted Camber (in)	Change in Predicted Camber (in)
1. Girders inverted and simply supported	- 2.6	- 2.6	- 2.4	- 2.4	0.14	-	0.34	-
2. Forms attached	- 7.7	- 5.1	- 7.5	- 5.1	0.91	0.77	1.08	0.74
3. Concrete poured	-19.4	-11.7	-21.3	-13.8	2.47	1.56	3.07	1.99
4. Extra weight added	-27.1	- 7.7	-28.8	- 7.5	3.34	0.87	3.93	0.86
5. Extra weight removed	-20.4	6.7	-24.4	4.4	2.95	-0.39	3.68	-0.25
6. Forms removed and unit turned 90°	- 8.2	12.2	-12.0	12.4	-	-	-	-
7. Unit turned additional 90° and set in Laboratory	0.0	8.2	- 2.6	9.4	1.95	-1.00	2.14	-1.54
8. Spreader girders set in place	3.4	3.4	0.0	2.6	1.57	-0.38	1.97	-0.17
9. Prior to first yield test	6.2	2.8	3.0	3.0	1.02	-0.55	1.39	-0.58
Sum of Changes		6.20		3.0		0.88		1.05

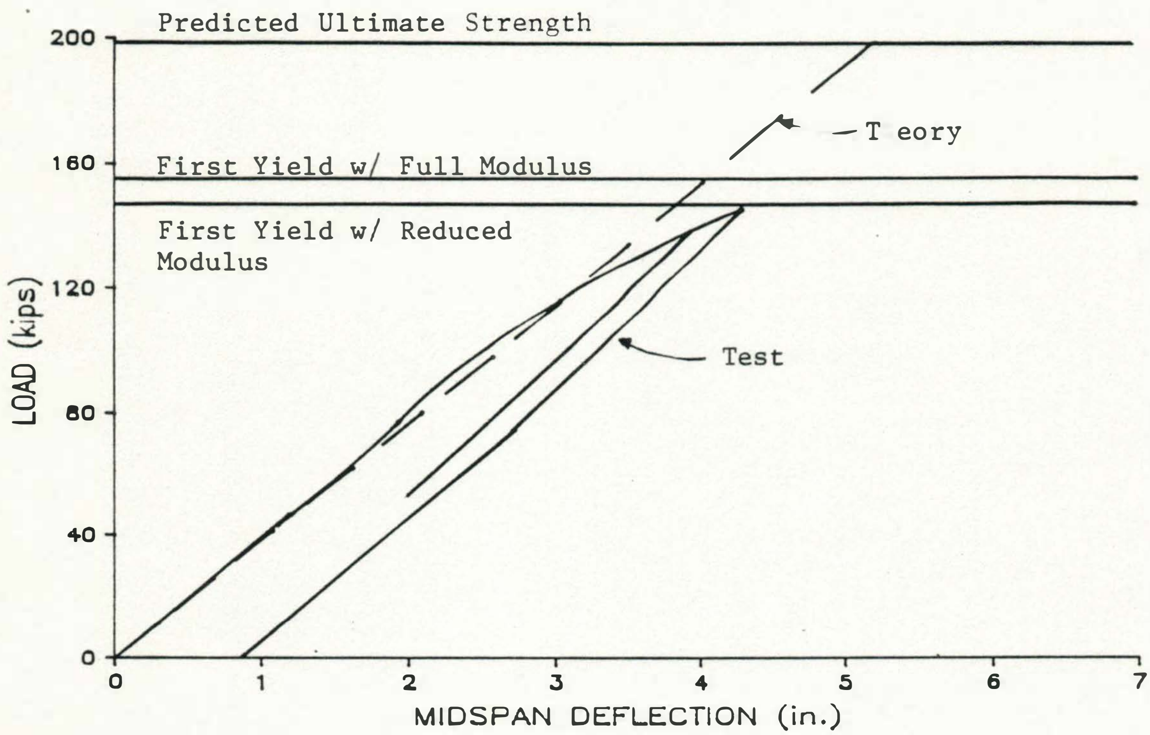

Figure 2.3 Load vs. Midspan Deflection (east girder)

The bottom horizontal line, labeled "First Yield w/ Reduced Modulus," corresponds to a load of 148 kips. This value was calculated using a reduced concrete modulus to compensate for creep and shrinkage effects. The next horizontal line, labeled "First Yield w/ Full Modulus," indicates a load of 156 kips. This value was calculated using the full concrete modulus, thus ignoring any effect of concrete creep or shrinkage. The top horizontal line corresponds to a load of 199 kips, which indicates the full plastic moment capacity of the bridge unit.

From the experimental curve given in Figure 2.3, it can be seen that the bridge unit yielded significantly earlier than predicted. If one defines first yield as when the experimental curve crosses the predicted elastic behavior line, then the yield load was approximately 125 kips for the east girder. The west girder showed similar behavior, with a first yield load of approximately 130 kips by the same definition. This reduction in the yield load below the predicted value of 148 kips was thought to be partially due to underestimated creep and overestimated prestresses.

Loading in the previous test was terminated at an applied load of 148 kips, including the weight of the spreader girder. This corresponds to the first yield load predicted using the reduced modulus method. The maximum displacement observed was 4.25 inches for the east girder and occurred at the maximum applied load of 148 kips. Loading was stopped at this point to save the bridge unit for possible resale. When the load was removed the unit only partially rebounded, sustaining a permanent deflection of 0.8 inches. This permanent deformation must be attributed to yielding of the unit. Yield lines were observed in the bottom flanges of the bridge unit girders, confirming that yielding of the girders contributed to the early inelastic behavior and permanent deflection observed. The yield lines observed were limited to the lower flanges and the lowest portion of the girder webs.

During the previous test of the second bridge unit, slippage was observed at the slab-girder interface. This slippage was noted to occur mostly near the load application points, with little slippage observed near the ends of the bridge unit.

CHAPTER III

CURRENT RESEARCH PROGRAM

3.1 Test Specimen Description

The current research program extends the previous testing of the second composite bridge unit by loading the specimen to failure. Dimensions, material properties, and slab reinforcement details of the bridge unit were presented in Chapter II. Transformed section properties of the specimen are shown in Figure 3.1.

3.2 Test Setup and Instrumentation

Loading and support conditions for the bridge unit were the same as for the previous test to first yield and are shown in Figure 3.2. Load was applied to an upper spreader girder by a 320 kip hydraulic actuator. The applied load was monitored using an electronic load cell placed between the actuator and the upper spreader girder. From the upper spreader girder, load was transferred laterally to points on the slab directly over the steel girders using two lower spreader girders. The bridge unit rested on neoprene pads at its ends which were supported by steel girders resting on cribbing.

Vertical displacements of each steel girder and horizontal slips between the slab and steel girders were monitored as shown in Figure 3.2. Vertical displacements were measured at the supports and midspan using displacement transducers. Relative horizontal slips between each steel girder and the concrete slab were measured at twelve locations (six on

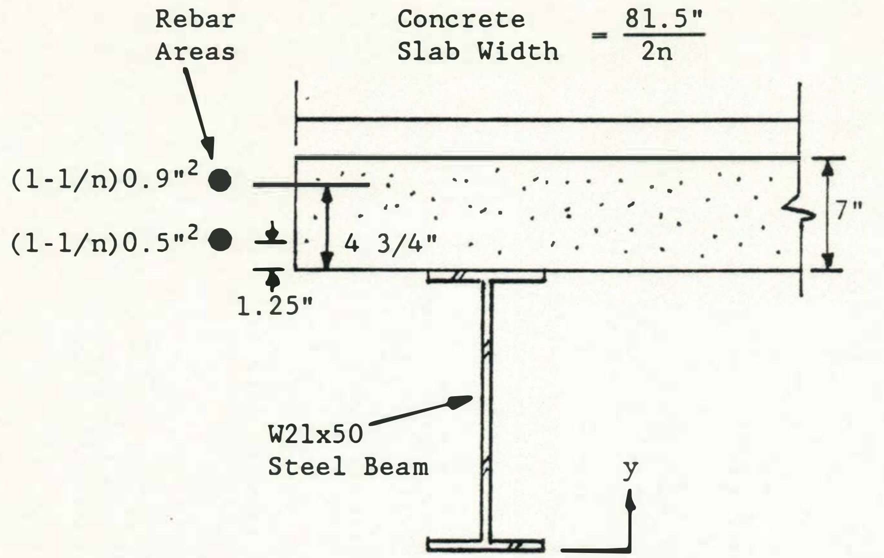

n = 5.44

	Properties of Half of Bridge Unit				
	$A(in^2)$	$y(in)$	$Ay(in^3)$	$Ay^2(in^4)$	$I_o(in^4)$
Concrete	52.44	24.33	1275.9	31041.8	214.12
Top Bars	0.73	25.58	18.8	480.9	-
Bottom Bars	0.41	22.08	9.0	198.9	-
Steel Beam	14.70	10.42	153.2	1596.1	984
Totals	68.3		1456.9	33317.7	1198.12

$$I_x = I_o + \Sigma Ay^2 = 34516.0 in^4$$

$$\bar{y} = \frac{\Sigma Ay}{\Sigma A} = 21.33 in$$

$$I/2 = I_x - A\bar{y}^2 = 3439.0 in^4$$

$I = 6878.0\ in^4$ (for complete bridge unit)

Figure 3.1 Transformed Section Properties of Bridge Unit (Reference 1)

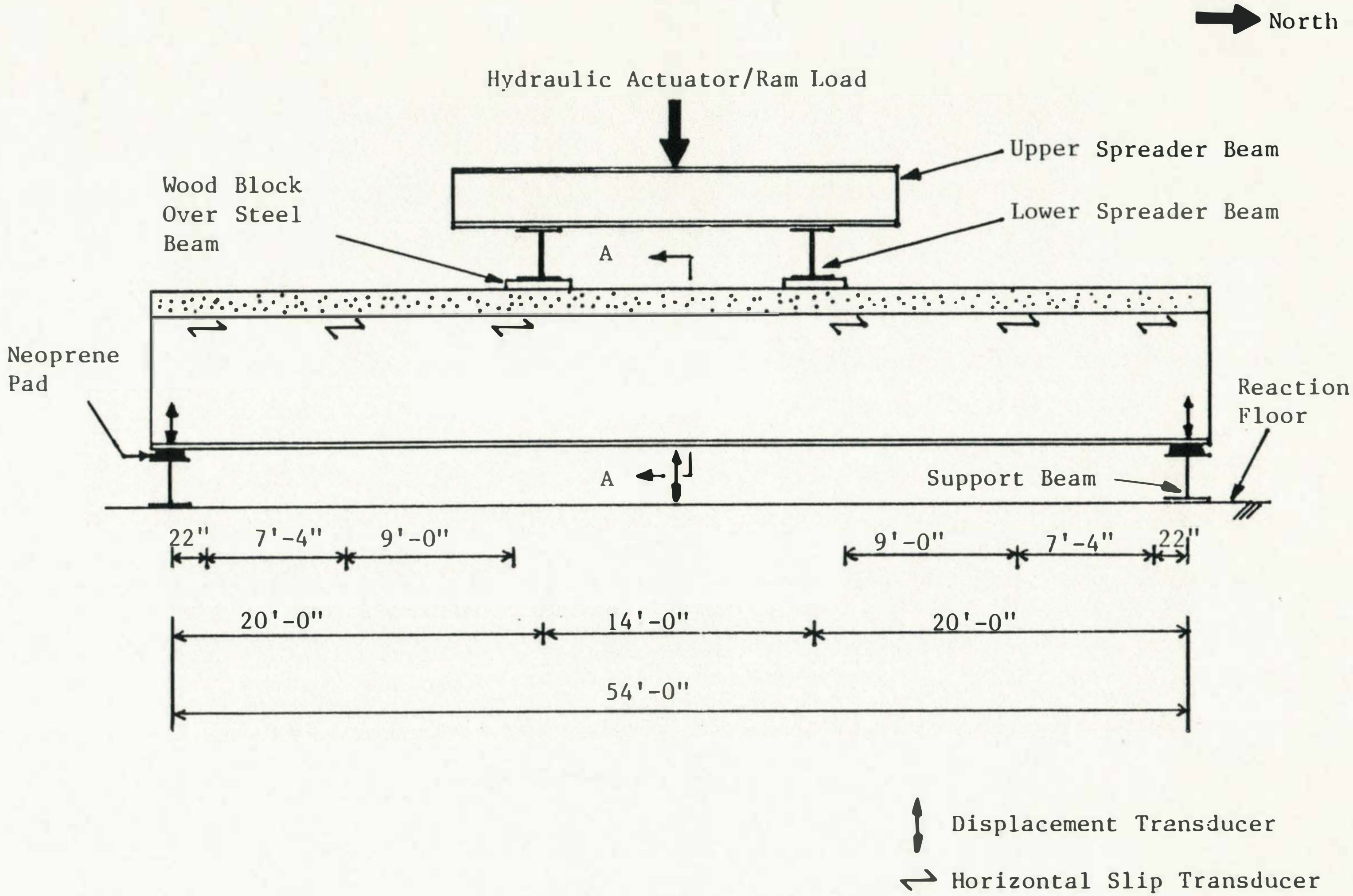

Figure 3.2 Loading Apparatus and Instrumentation

each girder). Displacement transducers were mounted on the steel girders and corresponding bearing blocks were mounted on the underside of the slab. At each location, the transducer and its bearing block were mounted at the same section so that the resulting gage length was zero.

Electrical resistance strain gages were used to measure longitudinal strains on the slab surface, slab reinforcement, and the steel girders. The gages were mounted on the bridge unit at midspan as shown in the section of Figure 3.3. Five gages were mounted on the slab surface to measure the lateral distribution of strain across the width of the slab. Existing gages on top and bottom slab bars were also monitored. Existing gages on the steel girders were used in conjunction with additional gages to record the distribution of strain over the depth of the girders. Gages were mounted on the tops and bottoms of the flanges and at three locations over the depth of the webs as shown in Figure 3.3.

Load, displacements, and strains were recorded using a microcomputer-controlled data acquisition system. A plot of ram load vs. midspan deflection was generated on the computer's monitor (in real time) and used to control the test. All data was stored directly onto disk for additional processing and plot generation after the test was completed.

3.3 Test Procedure and Results

The plots presented in this chapter were generated from data obtained on the east girder of the bridge unit. The unit behaved in a very symmetric manner, thus the results for only the east girder are presented here. Corresponding plots for the west girder are presented in Appendix A.

The test was conducted by applying increments of load until the ultimate load capacity was reached. At each increment, the load was allowed to stabilize before data was recorded in order to approximate static loading.

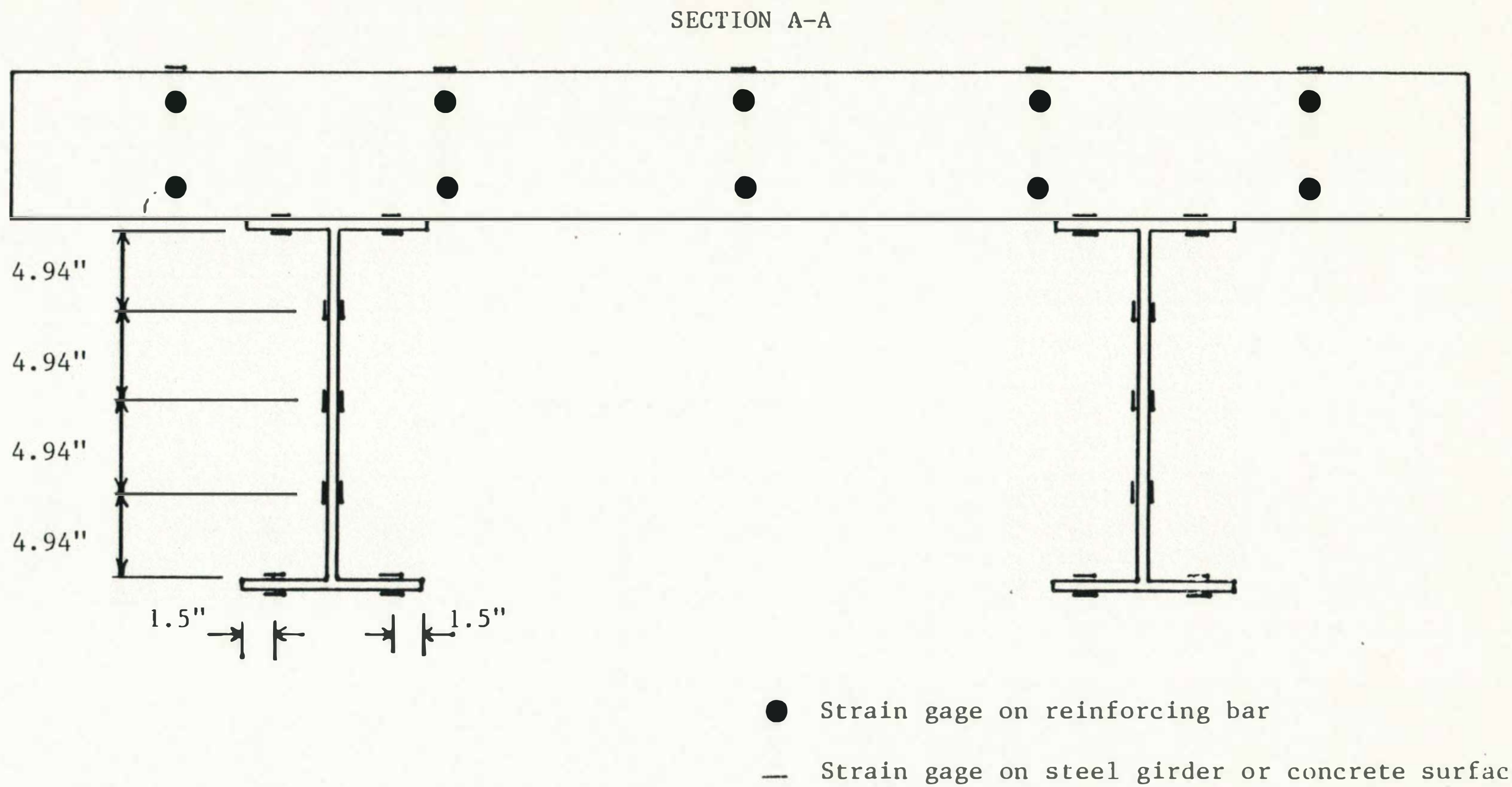

Figure 3.3 Strain Gage Locations at Midspan

The load vs. midspan deflection relationship for the bridge unit is shown in Figure 3.4. The dashed portion of the curve represents results of the previous test to first yield, while the solid portion represents loading conducted during the current study. The curve has been adjusted to include the effects of the spreader girders (self weight = 7.0 kips), but not the weight of the bridge unit. Thus, the load is the total externally applied load and the deflection is measured with respect to the deformed state of the unit due to its own weight.

As can be seen in Figure 3.4, the load-deflection curve of the current study picked up the path of the previous test. The unit was unloaded at a deflection of approximately 11 inches just prior to reaching the stroke limit of the hydraulic ram. A spacer block was then inserted to provide additional stroke and the test was continued to ultimate.

The bridge unit behaved in a very ductile manner, exhibiting large deflections up to failure. The unit is shown in Figure 3.5 at a stage near ultimate, with a midspan deflection of 16.5 inches. The maximum applied load was 224 kips with a corresponding maximum deflection of 18.6 inches. At this stage the slab suddenly failed in compression. Concrete spalling and delamination occurred over a slab depth of approximately 3 inches in the constant moment region near the load points. The spalling and delamination can be seen in the photo of Figure 3.6.

The variation of longitudinal strain over the depth of the unit at various load stages can be seen in Figure 3.7. The location of the neutral axis predicted from elastic theory was 0.33 inches above the slab-girder interface. Data from the strain gages indicated the measured neutral axis location was slightly below the interface. Plastic yielding of the girder occurred well up into the web at loads above 200 kips. As expected, the neutral axis shifted upward into the slab with increased plastic deformation of the girder.

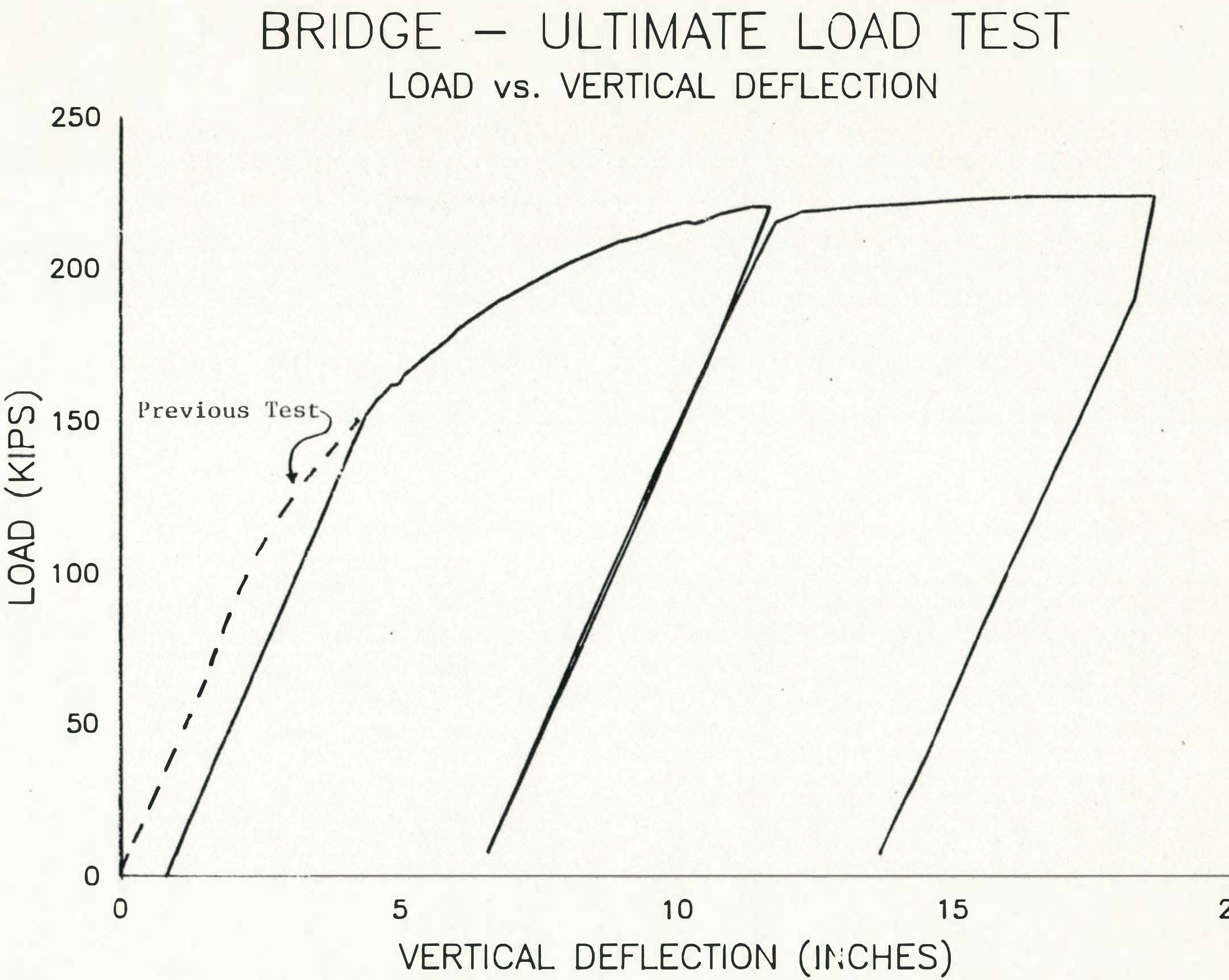

Figure 3.4 Load vs. Midspan Deflection (east girder)

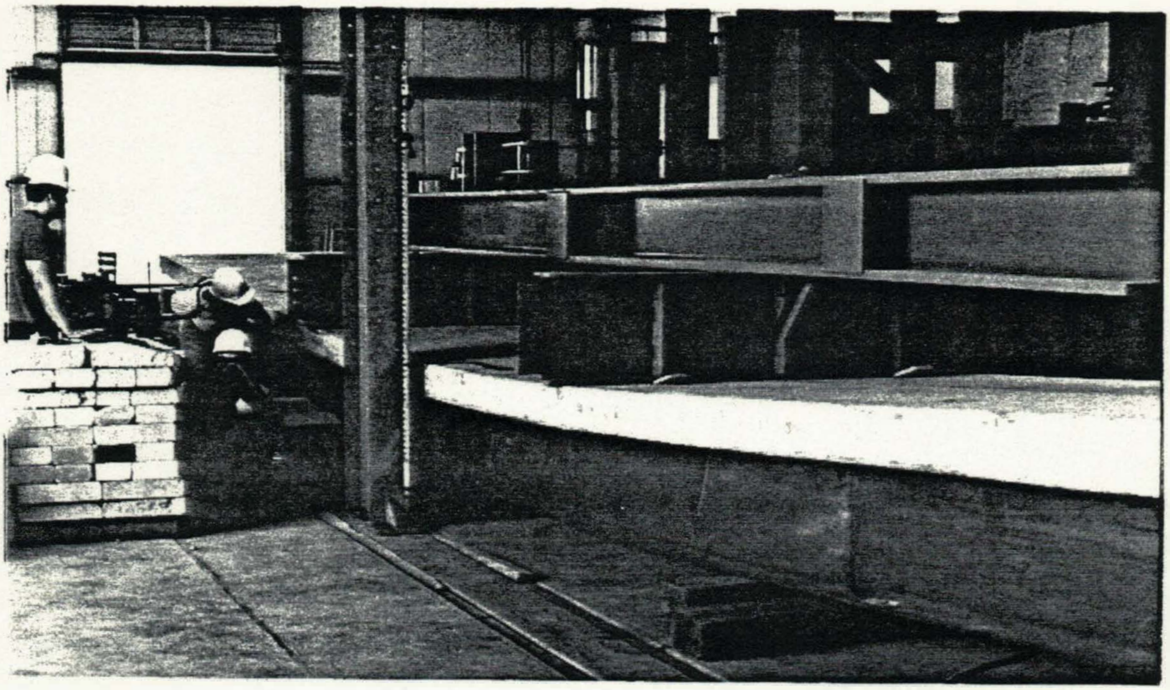

Figure 3.5 Bridge Unit During Test

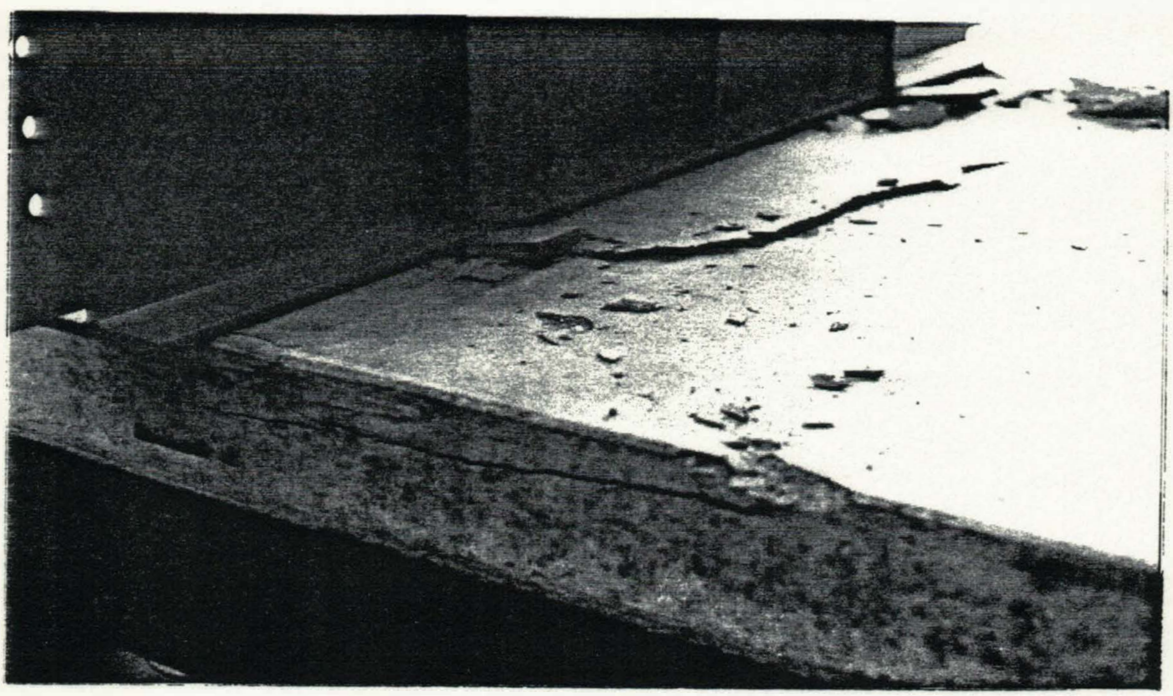

Figure 3.6 Compression Failure of Bridge Deck

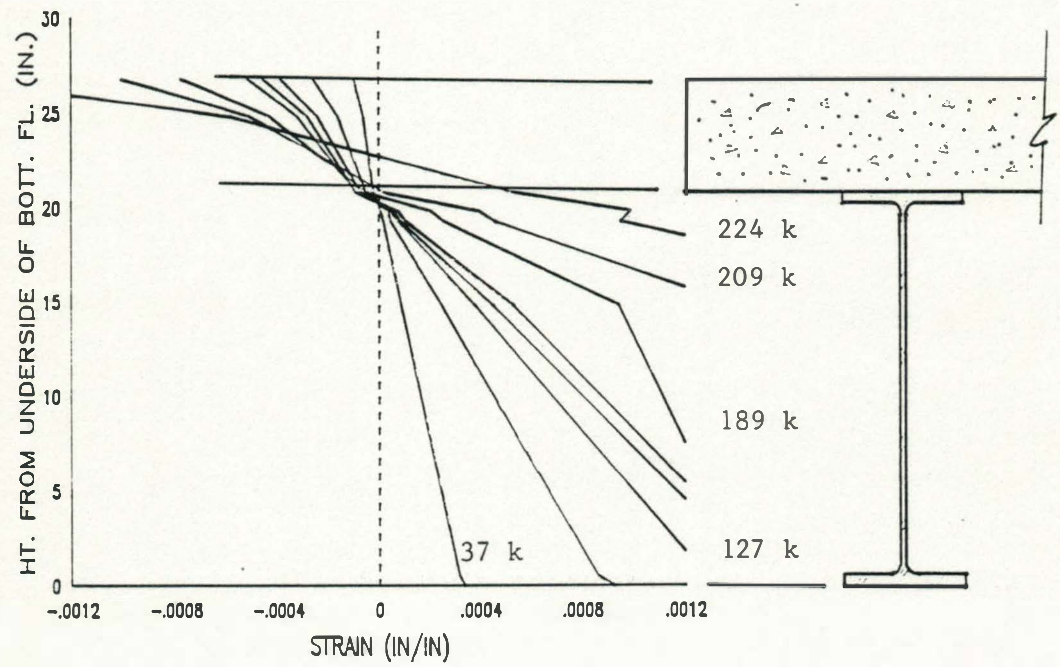

Figure 3.7 Strain vs. Depth at Various Loads

The variation in longitudinal strain across the top surface of the slab at various applied loads can be seen in Figure 3.8. One gage near the edge of the slab behaved erratically, thus its readings were omitted from the figure. There was essentially no difference in strains across the width during the test. This behavior could be expected given the large length to width ratio of the slab. The magnitudes of measured slab strain were also small. At ultimate, the average measured slab surface strain was 0.0018. However, the strain gages were located at midspan, and failure occurred near the load points where local compression was much higher. It is reasonable to expect that the slab surface strains near the load points were considerably larger than those measured at midspan.

Relative horizontal slip between the slab and steel girders are presented for several locations along the span in Figures 3.9 through 3.11. The plots of Figures 3.9, 3.10, and 3.11 refer to sections 1′-10", 9′-2" and 18′-2", respectively, inward from the supports. In general, magnitudes of slip and residual slip increased more rapidly in regions away from the supports. Although the shear is nearly constant in the regions between the supports and the load points, the moment increases toward the center of the span. Slips were observed to be largest in regions of combined high shear and moment, although the magnitudes were still small. As mentioned previously, the mode of failure of the unit was compression failure of the slab. This fact, in combination with the observed small slips, indicates shear transfer capacity at the interface was adequate. An explanation for the increase in slip in regions of high moment is presented in Chapter IV.

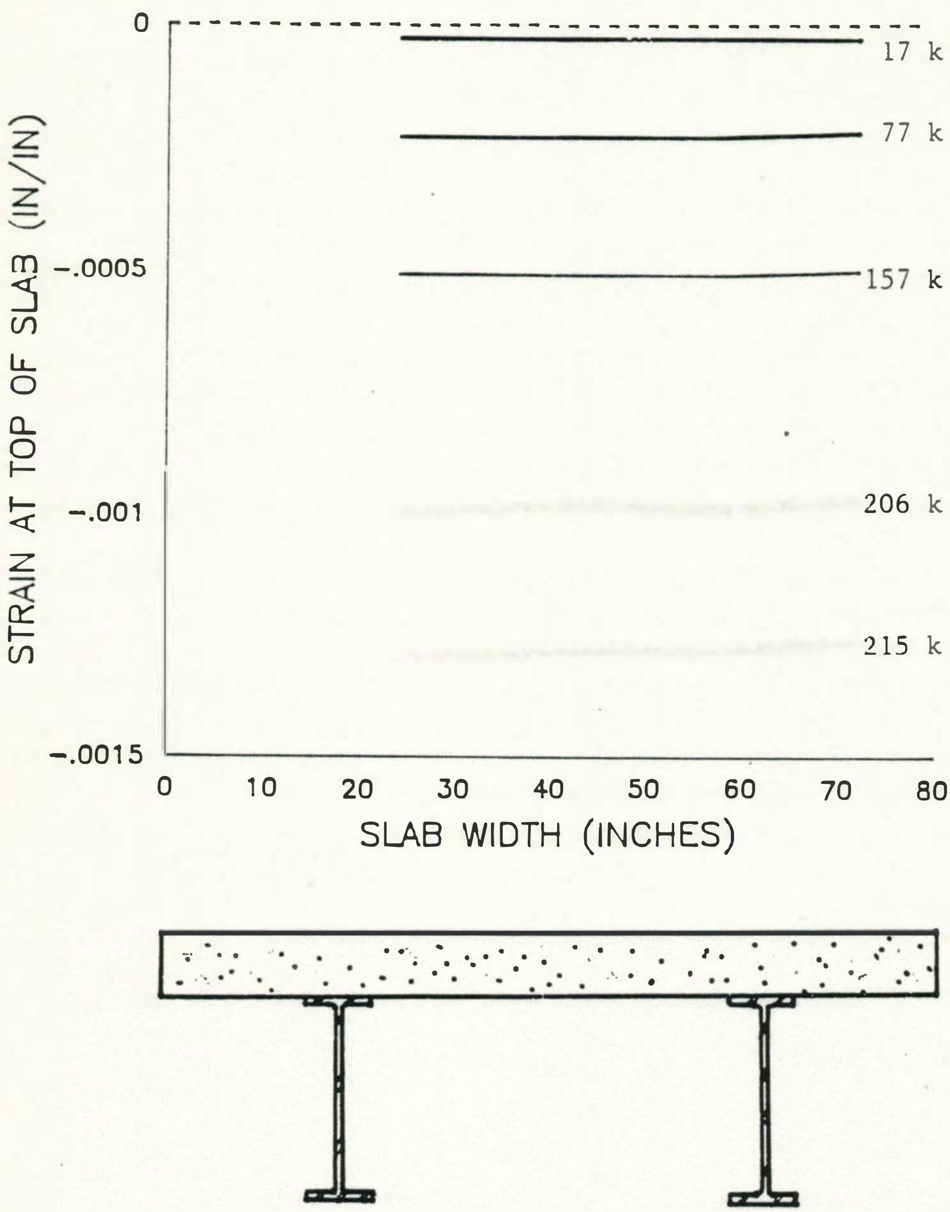

Figure 3.8 Strain Distribution Across Slab at Various Loads

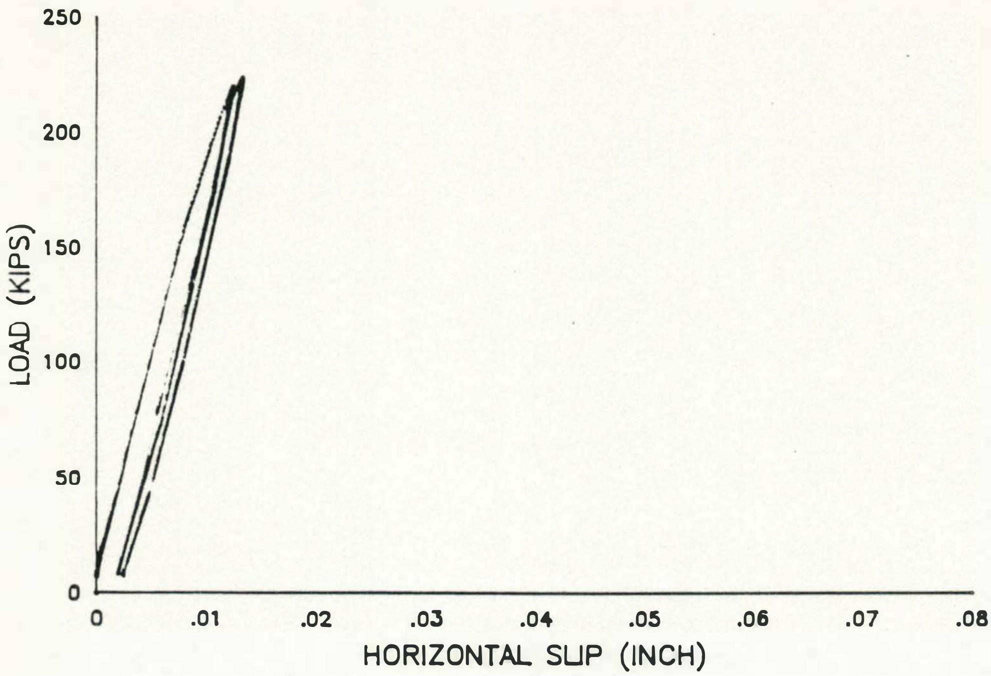

(a) 1'-10" from north support

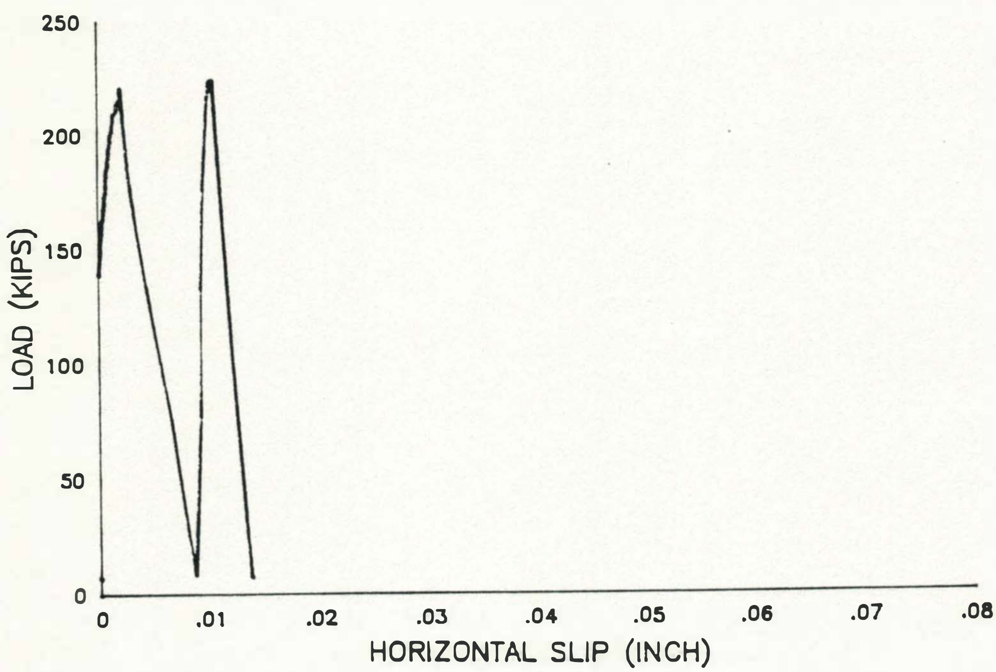

(b) 1'-10" from south support

Figure 3.9 Slip at Slab-Girder Interface (east girder)

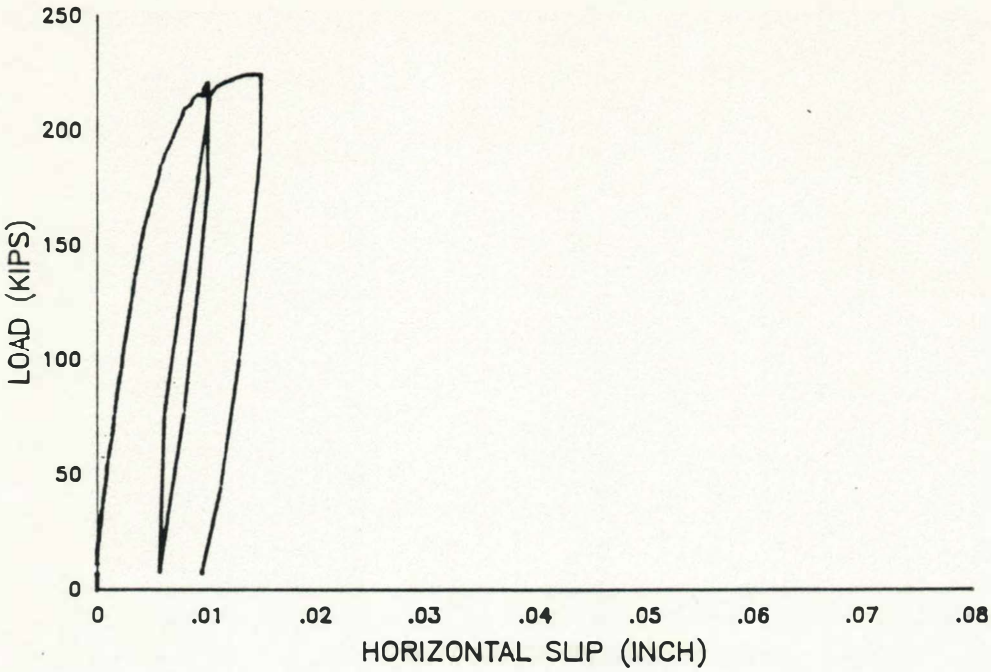

(a) 9'-2" from north support

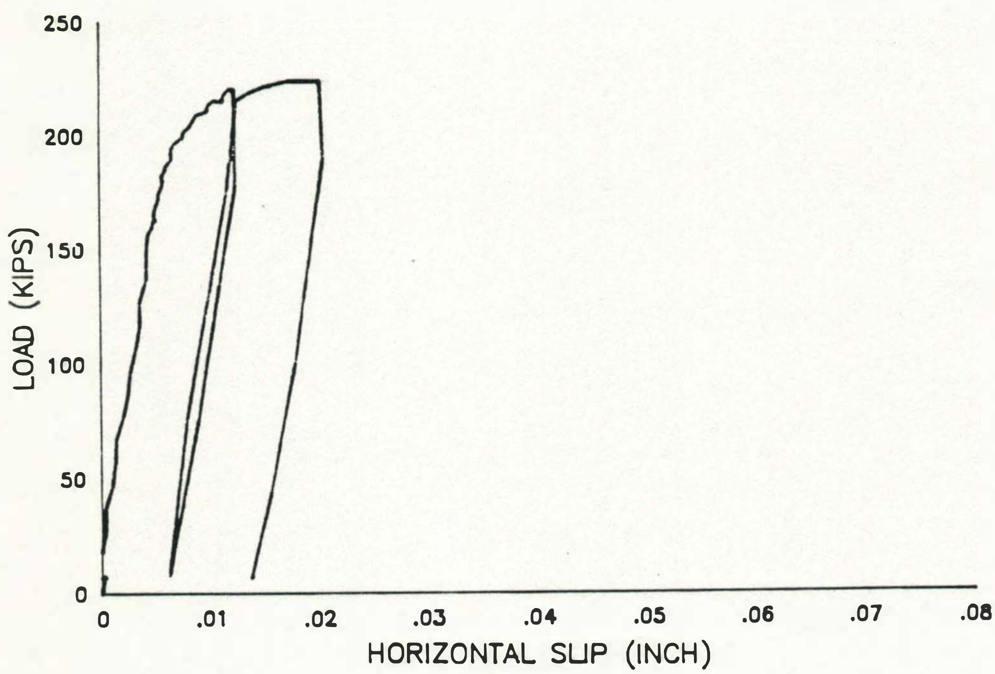

(b) 9'-2" from south support

Figure 3.10 Slip at Slab-Girder Interface (east girder)

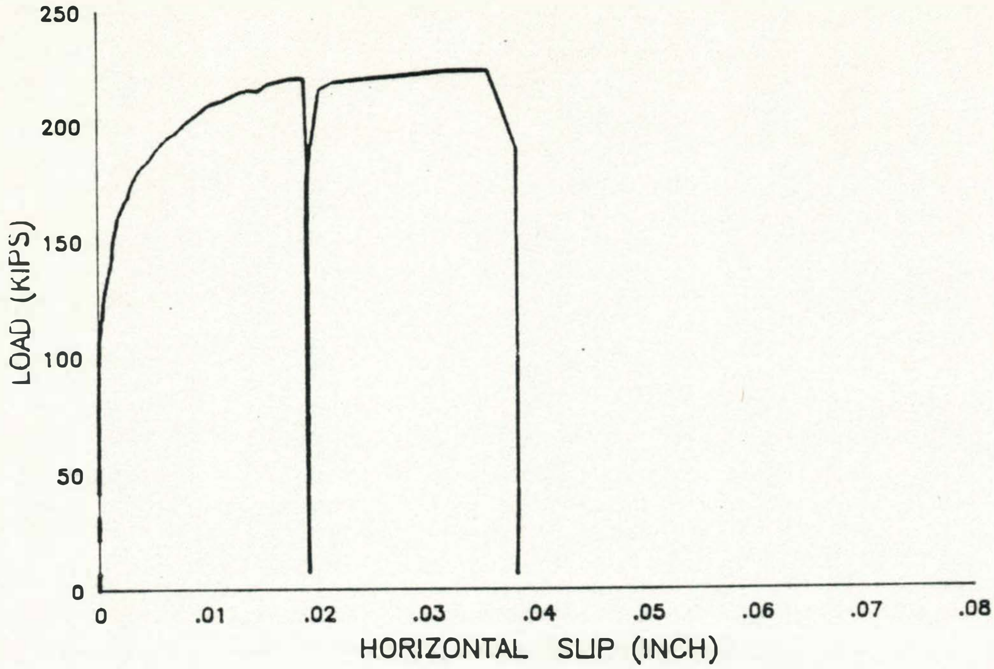

(a) 18'-2" from north support

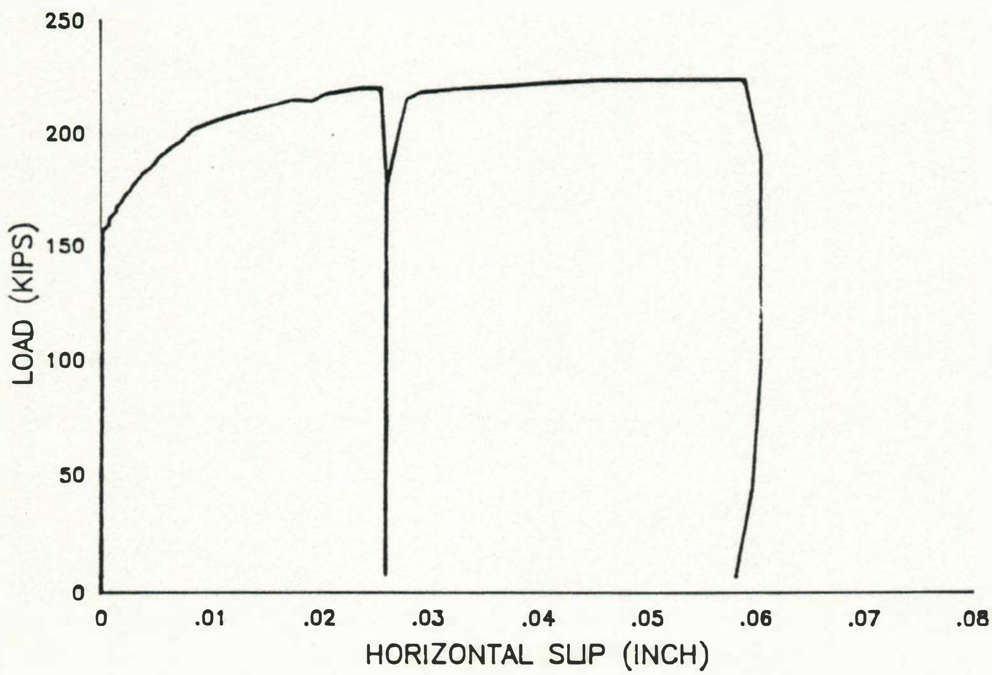

(b) 18'-2" from south support

Figure 3.11 Slip at Slab-Girder Interface (east girder)

CHAPTER IV

ANALYSIS OF TEST RESULTS

4.1 Ultimate Load Capacity

The bridge unit resisted a maximum applied load of 224 kips during the test which corresponds to a maximum applied moment of 2240 ft-kips. The maximum moment due to the self-weight of the bridge unit is 250 ft-kips, resulting in a maximum moment resisted during the test of 2490 ft-kips.

The capacity of the bridge unit was predicted to be 2240 ft-kips. By subtracting the self-weight moment of 250 ft-kips and then considering the shape of the moment diagram due to the applied load, a predicted capacity of 199 kips applied load is obtained. This prediction was made using the Whitney stress block for the compression region of the concrete deck and the yield or elastic stress in the steel girders and reinforcing bars, depending on the strains at each location. Material properties used in this prediction include measured yield stress of the steel girders and reinforcing bars as reported in Table 2.1. The concrete compressive strength was taken as 7,400 psi to account for additional strength gain since the last cylinders were tested.

From these numbers, it can be seen that the bridge resisted 11% more moment than predicted using measured properties. This corresponds to a 13% increase in live load capacity. The most likely cause of this excess capacity is strain hardening in the bottom flange region of the girders.

The nominal capacity of the bridge unit is calculated to be 1880 ft-kips. Yield strengths of 50 and 60 ksi for the girders and reinforcing bars, respectively, and a concrete compressive strength of 5000 psi were used in this analysis. Comparing this capacity to the experimental results, the specimen resisted 32% more moment than the nominal capacity used in design.

4.2 Yield Load Capacity

One of the observations of the previous test program was that the bridge unit yielded earlier than expected. This behavior can be seen in Figure 2.3. If one assumes first yield to occur when the experimental curve crosses the elastic behavior line, the bridge unit started yielding at an applied load of approximately 125 kips. This is significantly less than the load of 146 kips calculated using the reduced modulus method to account for creep and shrinkage.

A more detailed analysis of the expected first yield load using the strain gage data from the bottom girder flanges reported in Table 2.2 is as follows: The bottom girder flange stress when the bridge unit was first placed in the laboratory was 0.0 ksi. Immediately after the spreader beam was installed, the stress determined from strain measurements was 3.4 ksi. The stress in this same location was 6.2 ksi after the 500,000 cycles of fatigue loading and just before starting the first yield test. The difference between the stresses before and after the fatigue loading (6.2 - 3.4 = 2.8 ksi) is attributed to creep and shrinkage. The elastic stress range still available to resist bending is then 58.0 - 2.8 = 55.2 ksi. Multiplying this stress range by the elastic section modulus gives an expected elastic moment capacity of 1483 ft-kips which corresponds to an applied load of 148.3 kips. It is noted that this is close to the first yield load predicted using the reduced modulus method.

Both of these first yield load predictions significantly overestimated the experimentally determined yield load. Both predictions considered creep and shrinkage, but neither considered the effects of residual tensile stresses in the bottom flanges of the bridge girders. The presence of tensile residual stresses is usually not considered in the design of steel beams as it has no affect on the ultimate moment capacity, but it will cause the first yield moment to be reduced.

Residual stresses of rolled steel beams have been investigated and reported by Huber and Beedle [4] and Beedle and Tall [5]. While compressive residual stresses were the primary focus of these articles, residual tensile stresses were observed in the center of flanges. These stresses were reported as high as 24.2 ksi, with 5 to 15 ksi suggested as an average tensile residual stress. If one assumes a tensile residual stress of 10.0 ksi in the bottom girder flanges, then the available elastic range becomes 58.0 - 2.8 - 10.0 = 45.2 ksi. This gives an available elastic moment capacity of 1215 ft-kips which corresponds to an applied load of 121.5 kips. This agrees well with the experimentally determined first yield load observed in Figure 3.4.

4.3 Slippage at Slab-Girder Interface

Another topic of interest is the slippage measured at the slab-girder interface. These movements are presented in Figures 3.9, 3.10, and 3.11 for the east girder and Figures A.2, A.3, and A.4 for the west girder. From these figures it can be seen that more elastic slip occurred near the bridge unit ends, but little permanent deformation occurred there (see Figures 3.9 and A.2). Near the loading points little elastic slip was measured, but significant permanent slip occurred at higher loads. This same behavior was observed in the first yield load test [1]. The differences in the behavior between measurements close to the bridge unit ends and near the loading points is of interest, as the shear forces are almost the same at each location.

The lack of elastic slippage near the loading point may be explained by the fact that the load was applied to the top of the slab, thus clamping the slab to the girder. The resulting frictional shear force between the slab and girders aids the shear connectors in resisting the horizontal shear forces.

The much larger permanent slips measured near the load points are believed to be caused by an increase in the horizontal shear force at the slab-girder interface when the girder partially yields due to bending. This mechanism may be explained with the aid of the stress and resulting force diagrams of Figure 4.1. For the purpose of discussion, the neutral axis is assumed to occur at the slab-girder interface. Figure 4.1 (a) shows the normal stresses due to bending along with an increment of these stresses for a composite unit which behaves elastically. The increment in bending stresses (shown shaded in the figure) is due to the increment of moment caused by the shear force acting over the length of the section considered (V times dx). This moment is resisted by a couple which consists of the resultant compressive force (ΔC) and the resultant tensile force (ΔT) acting at a moment arm of z. The shear connectors in this length of girder (dx) must resist the force in this couple (ΔC or ΔT).

Now consider the same shear force applied concurrently with sufficient moment to cause partial yielding of the girder as indicated in Figure 4.1 (b). The same shear force V will cause the same increment of moment, V times dx. Because the lower portion of the girder is now yielded due to the moment, the increment of bending stresses (shown shaded in the Figure) occurs over a shallower section. Because the moment arm of the couple, z', is much shorter, the horizontal forces to be resisted ($\Delta C'$ and $\Delta T'$) are proportionally increased. This larger horizontal shear force ($\Delta C'$ or $\Delta T'$) must be resisted by the shear connectors over the same (dx) length of girder.

From this discussion, it can be concluded that flexural yielding of the girder will cause larger shear forces in the shear connectors in that

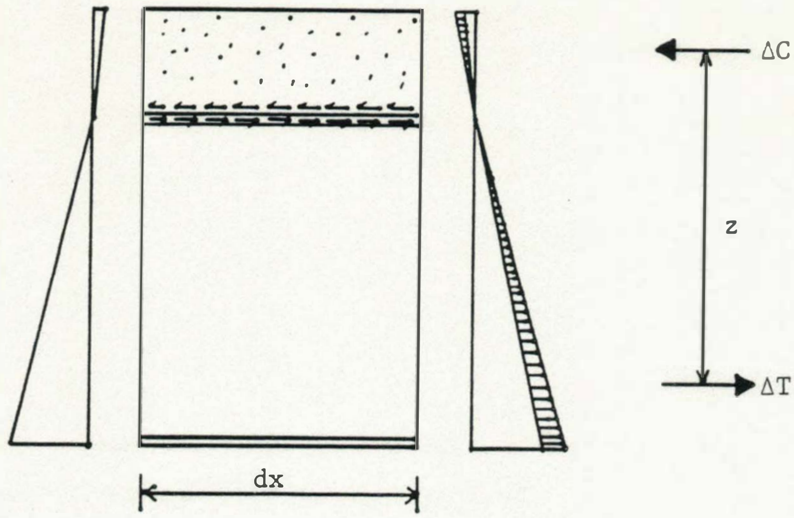

a) stress distribution and resultant shear forces before beam yielding

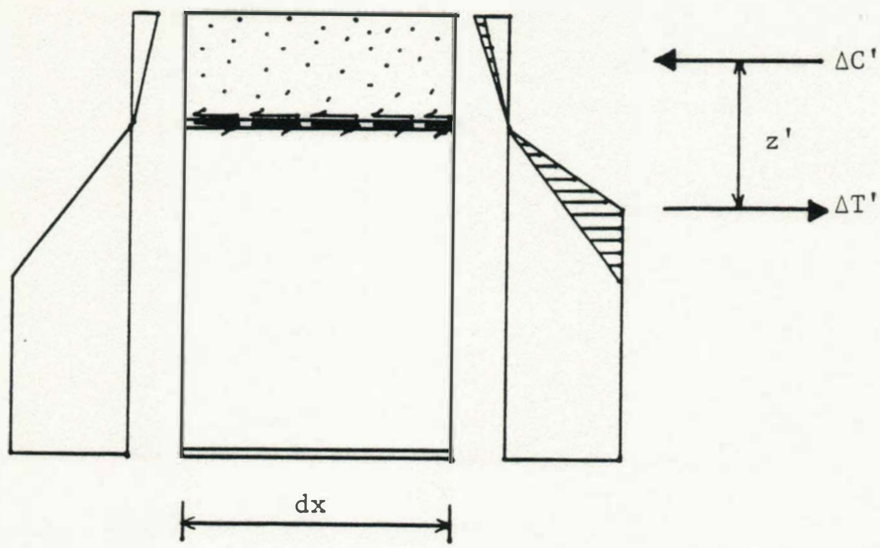

b) stress distribution and resultant shear forces in a partially yielded beam

Figure 4.1 Shear Connector Forces Required for Composite Action region than predicted using elastic analysis. This conclusion is supported by the load at which permanent slippage started, which is close to the yield load for the bridge unit. The shear connectors near the bridge unit ends showed little slippage because there was no girder flexural yielding at that location.

It is noted that the normal stress distributions used in Figure 4.2 do not include the effects of prestressing. This makes no difference to the increment of normal stress for the elastic stress distribution in part (a). Prestressing will modify the shape of the normal stress increment in part (b), but there will still be a reduced moment arm which results in increased shear forces on the shear connectors.

The increase in shear force discussed in this section is not of concern if the shear connectors have been designed for the case of full plastic moment capacity of the composite section. This increase is also not of concern if designs are limited to first yield, as the increase in shear forces only occurs when yielding occurs. If shear connectors are designed on the basis of elastic shear flow, then the shear caused by the prestressing forces should also be included in the analysis. This does not appear to be a problem with bridge design, as the AASHTO specification [3] uses an ultimate strength approach to shear connector design.

CHAPTER V

DESIGN IMPLICATIONS USING THE AASHTO SPECIFICATION

5.1 Service Load Design Method

The provisions for designing composite girders using the service load design method (allowable stress design) are given in section 10.38 of the AASHTO specification [6]. Basic provisions of this portion of the specification and implications of each provision for the design of prestressed composite girders are as follows:

1. Values of the ratio between the modulus of elasticity of steel and concrete (the modular ratio) are dependent upon the concrete cylinder strength and are given in a table. This assumption is applicable to the prestressed composite girders without change.

2. Creep due to concrete stresses resulting from long-term (dead) loads is accounted for by using a modular ratio multiplier of 3. This method is known as the effective modulus method and accounts for creep by calculating stresses and deflections using composite section properties based on a reduced concrete modulus. It is an alternative to Branson's method, which was discussed in the previous report [1]. It was noted in the previous report that while Branson's method provides a better qualitative understanding of the effects of creep and shrinkage, it is not necessarily more accurate. Also, Branson's method requires knowledge of concrete creep and shrinkage strains which are functions of variables such as

temperature and humidity during construction, which are usually unavailable to the designer. For these reasons, the effective modulus method is often used in design. To use the effective modulus method in the design of these prestressed composite bridge girders, prestresses must be treated as additional long-term (dead load) stresses.

3. The effective width of concrete slabs is limited by functions of span length, deck thickness, and beam spacing. These functions are the same as used by the American Institute for Steel Construction in their specification for steel buildings. This provision is applicable to prestressed composite girders without change.

4. Shear connectors between the steel beams and slab are designed for fatigue using elastic shear flow calculations and the shear due to live and impact loads only. This provision implies that only the cyclic variation in shear stress due to live and impact loads is important in the design of shear connectors to resist fatigue. As live load stresses are still elastic in the prestressed composite girders, this provision is applicable the same as for non-prestressed girders. It should be noted that the prestressing results in additional "dead load" shear stresses above those found in similar non-prestressed girders. This effectively increases the mean shear force to be resisted by the connectors. This increased mean connector stress does not enter into the AASHTO design procedure.

5. Shear connectors between the steel beams and slab are also required to develop the ultimate moment capacity of the section. This provision is unchanged for the prestressed composite girder because the ultimate moment capacity of the section is unchanged.

As an example of the service load design method, the prestressed composite bridge unit is analyzed in Appendix C using nominal design values. Also included are operating and inventory rating calculations as defined in the AASHTO Manual for Maintenance Inspection of Bridges (7).

5.2 Strength Design Method

The provisions for designing composite girders using the strength design method (load factor design) are given in section 10.50 of the AASHTO specification [6]. Basic provisions of this portion of the specification and implications of each provision for the design of prestressed composite girders are as follows:

1. Check for "compactness" to determine if the steel section is capable of developing its full plastic moment capacity.

2. If the steel section is compact (or if the top steel flange is not required to yield in compression), the strength calculations are based on the ultimate capacity of the plastic section. These calculations are unaffected by prestressing. This case is the usual condition for composite beams manufactured using rolled steel shapes, which are almost all compact.

3. If the steel section is noncompact, the maximum strength is limited to the moment at first yielding. These calculations include the effects of prestressing in the determination of stresses due to factored loads. The load factor for dead loads is applicable to the prestressing effects.

4. All composite girders are to be checked for the overload condition as specified in section 10.57 of the AASHTO specification [6]. This provision requires calculation of stresses due to factored loads, which are checked against 0.95 F_y. The effects of prestressing must be included in the determination of these stresses.

As an example of the strength design method, the prestressed composite bridge unit is analyzed in Appendix C using nominal design values. Also included are operating and inventory rating calculations as defined in the AASHTO Manual for Maintenance Inspection of Bridges (7).

CHAPTER VI

SUMMARY AND CONCLUSIONS

A full-scale composite prestressed bridge unit was tested to ultimate in the laboratory. The following summary and conclusions can be drawn from results of the test.

1. The bridge unit carried an applied load slightly above its predicted ultimate capacity. The maximum applied load of 224 kips was 13% above the predicted capacity of 199 kips. The most likely cause of this excess capacity is strain hardening in the bottom flange region of the girders. It is commonly accepted that the ultimate moment capacity of a ductile flexural member is not affected by prestressing.

2. The unit behaved in a very ductile manner, exhibiting large deflections up to ultimate. A maximum deflection of 18.6 inches in the 54 ft. span was measured just prior to failure. The mode of failure was spalling and delamination of the slab near the load points. Measured strains indicated that yielding occurred over nearly the full depth of the webs.

3. The applied load at first yield (from a previous test) was somewhat lower than predicted. The reduced yield load can likely be attributed to the presence of residual rolling stresses in the bottom flanges of the girders. The presence of these stresses is of no more concern for the bridge unit tested than for any steel girder.

4. Measured horizontal slips at the slab-girder interface were very small. The maximum recorded residual slips were approximately 0.06 inches. These maximum slips occurred only in regions where yielding of the girders had extended well into the webs.

REFERENCES

1. Densford, T., and Murray, T., "Experimental Study of Two Prestressed Steel Beam-Concrete Slab Bridge Units". Research Final Report, FSEL/ODOT 86-02 submitted to Research Division Oklahoma Department of Transportation, Fears Structural Engineering Laboratory, August 1986.

2. Densford, T., and Murray, T., "Experimental Study of Two Prestressed Steel Beam-Concrete Slab Bridge Units". Executive Summary, FSEL/ODOT 87-02 submitted to Research Division Oklahoma Department of Transportation, Fears Structural Engineering Laboratory, August 1986.

3. Standard Specification for Highway Bridges. 12th Edition, American Association of State Highway Officials, 1977.

4. Huber, A.W., and Beedle, L.S., "Residual Stress and the Compressive Strength of Steel," Final Report on a Pilot Program, Welding Journal, Vol. 33, No. 12, December, 1954, p 589-s.

5. Beedle, L.S., and Tall, L., "Basic Column Strength," Journal of the Structural Division, ASCE, Vol. 86, No. ST7, July, 1960.

6. Standard Specification for Highway Bridges. 13th Edition, American Association of State Highway Officials, 1986.

7. Manual for Maintenance Inspection of Bridges, American Association of State Highway Officials, 1983 (with 1989 revisions).

APPENDIX A

TEST RESULTS FROM WEST GIRDER

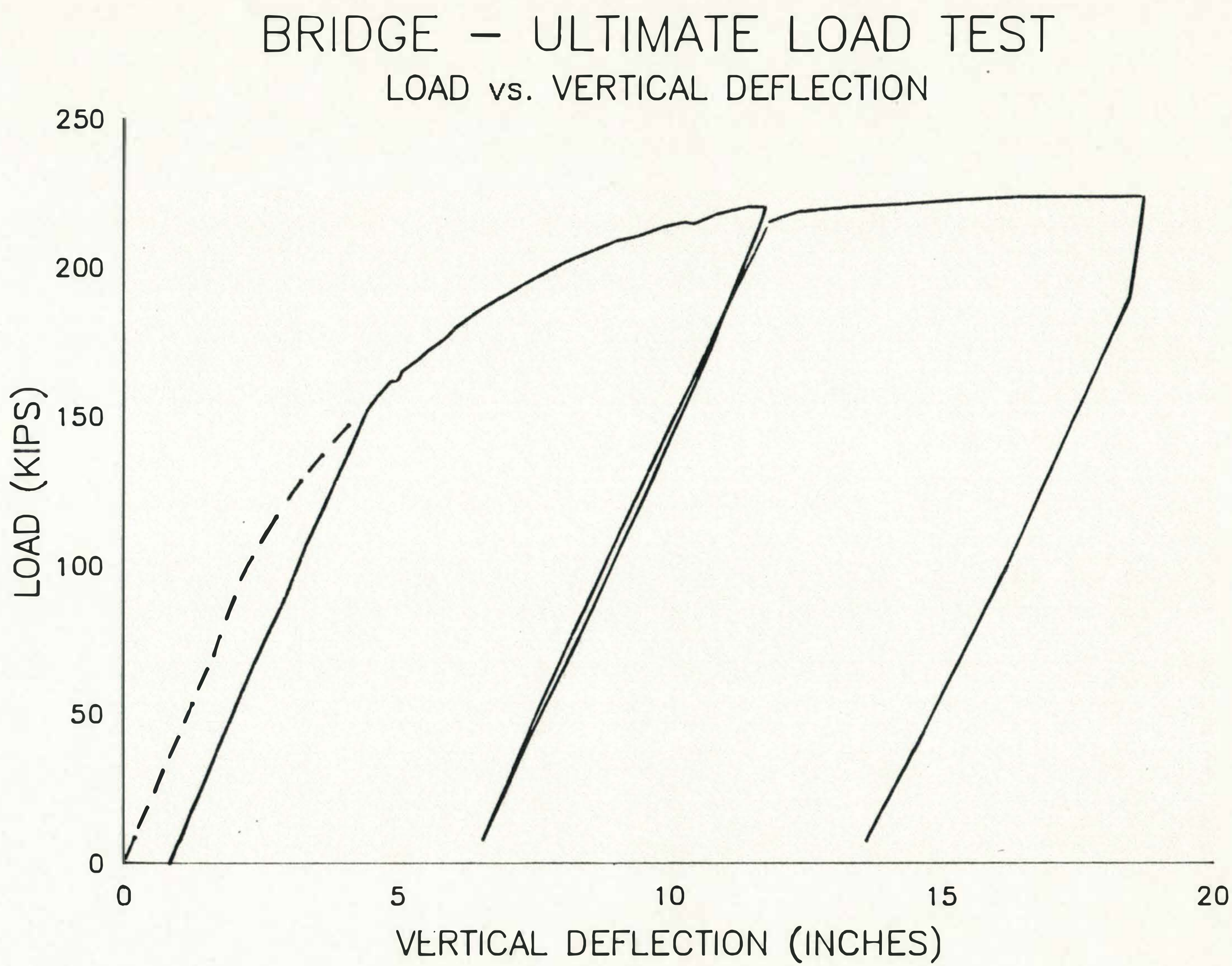

Figure A.1 Load vs. Midspan Deflection (west girder)

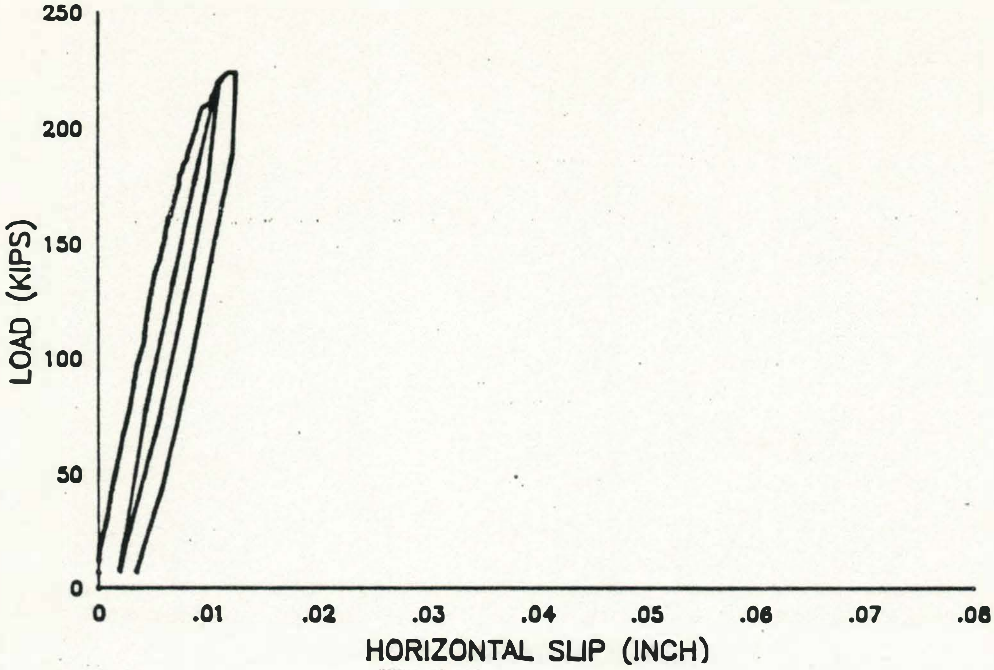

(a) 1'-10" from north support

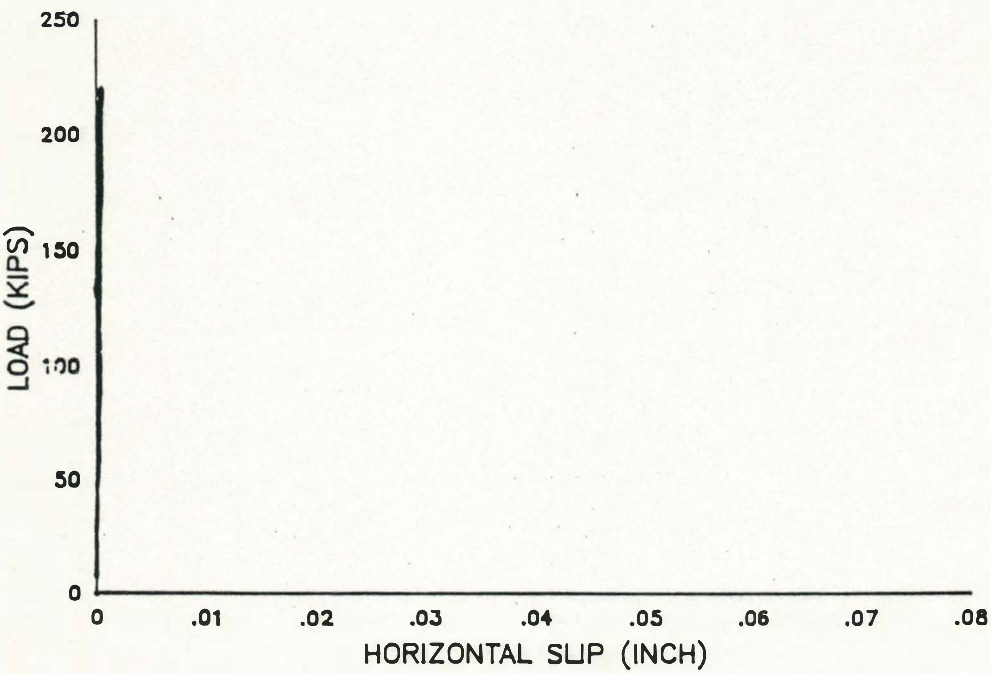

(b) 1'-10" from south support

Figure A.2 Slip at Slab-Girder Interface (west girder)

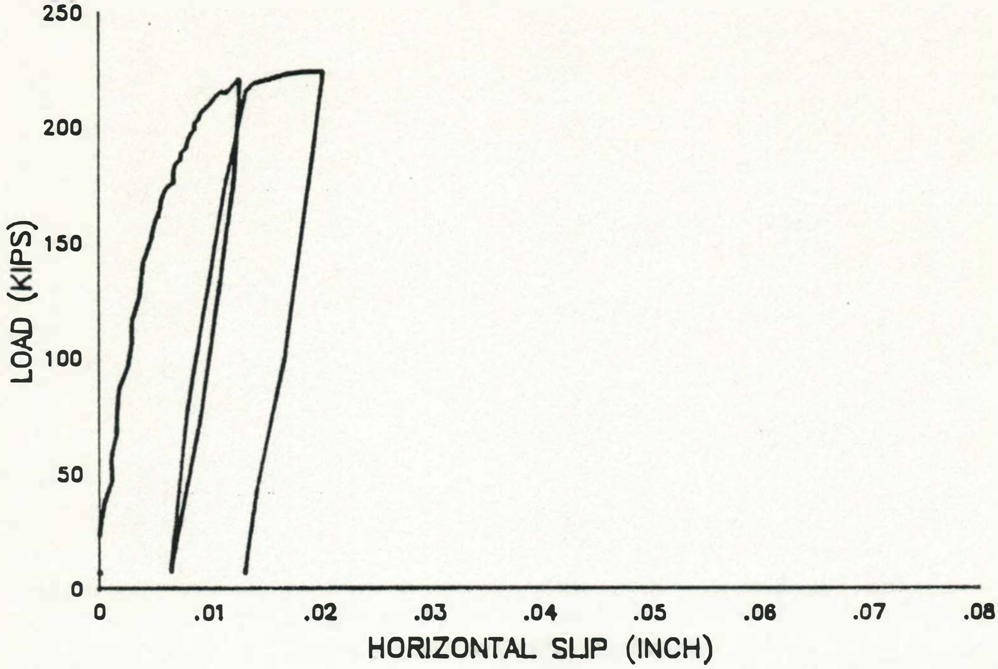

(a) 9'-2" from north support

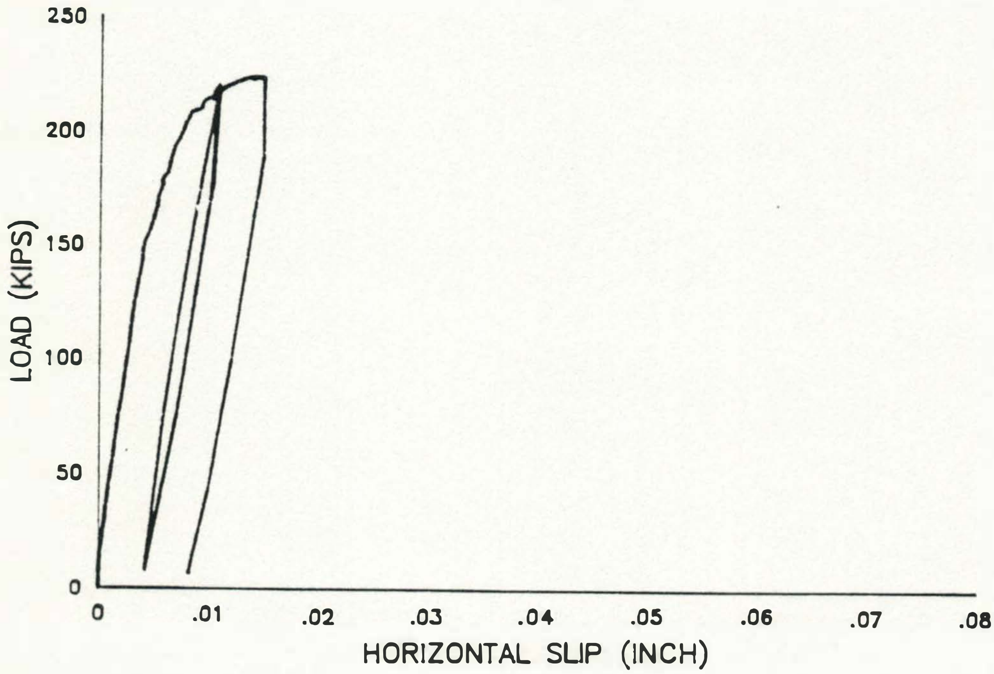

(b) 9'-2" from south support

Figure A.3 Slip at Slab-Girder Interface (west girder)

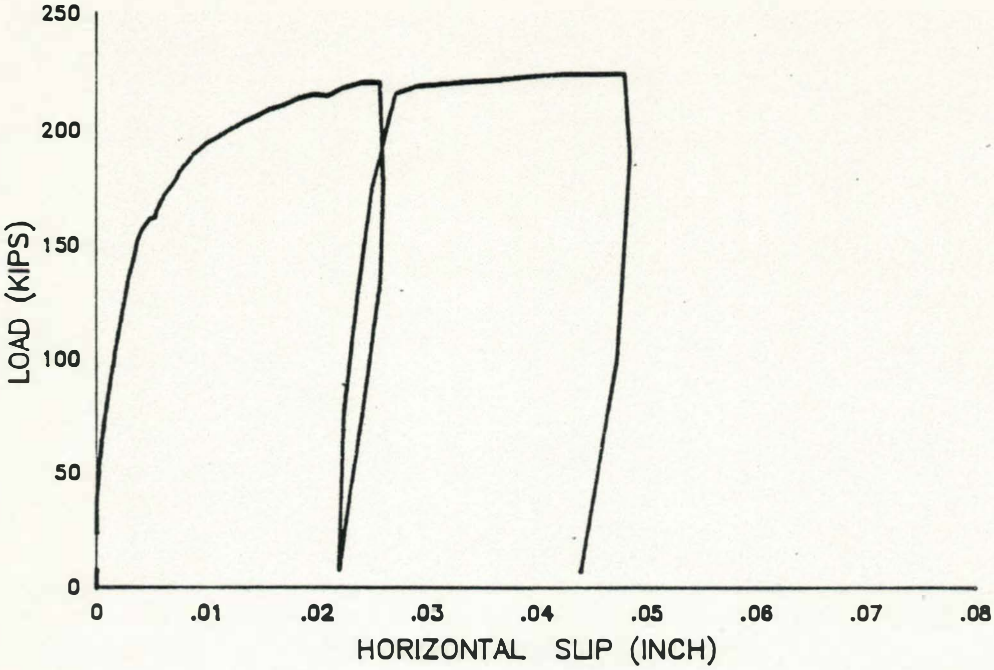

(a) 18'-2" from north support

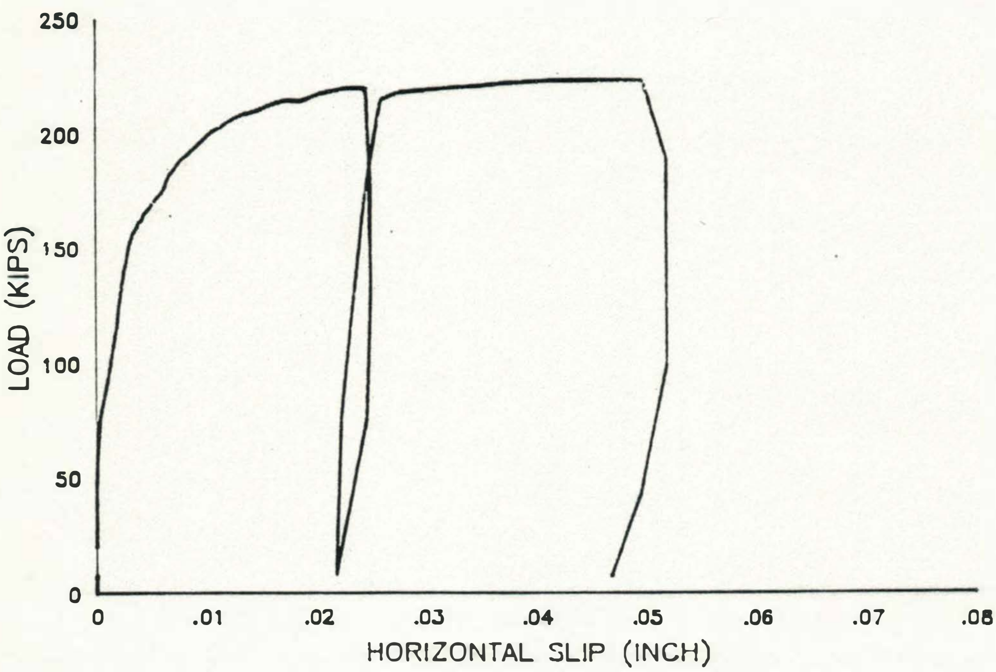

(b) 18'-2" from south support

Figure A.4 Slip at Slab-Girder Interface (west girder)

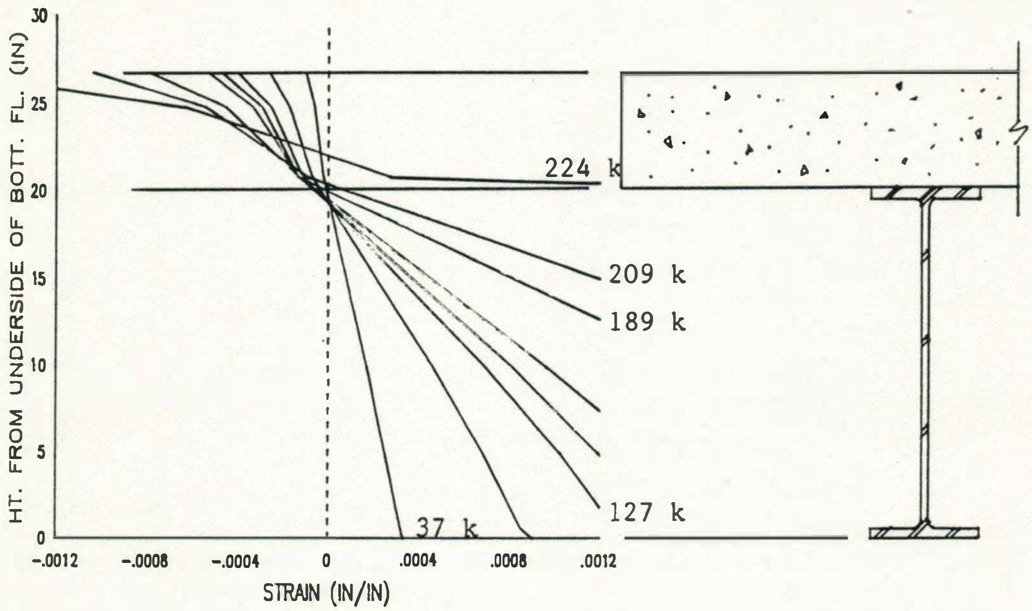

Figure A.5 Strain vs. Depth at Various Loads (west girder)

APPENDIX B

ELASTIC ANALYSIS OF TEST UNIT

APPENDIX B

In this appendix, the calculations used to predict construction stresses, including the effects of creep and shrinkage are presented. These calculations use simple flexure theory with the properties of the bare steel beams before the concrete deck has cured and the properties of the composite section after the concrete deck has cured. Material properties for the section are given in Table 2.1. Transformed section properties of the unit are given in Figure 3.1.

In this type of construction, gravity loads including the weight of steel beams, form, and wet concrete are applied to the inverted steel beams during construction. After the concrete has cured, the composite section then resists the subsequent loads, including stresses from turning the unit upright. This process results in locked in stresses (prestress) which raises the applied load required to cause first yield of the beams. This increase in yield load will raise the design capacity of the bridge unit if the controlling design criteria is first yield. If the controlling design criteria is ultimate capacity, then the prestressing will have no effect on the design capacity of the unit, as prestressing has no effect on the ultimate capacity of these units.

Creep and shrinkage of the concrete in these units will reduce the prestressing, causing a reduction in the yield load. This will occur during the time the concrete is curing (shrinkage) and later due to long term stress on the concrete (creep). Because these effects reduce the yield load of the unit, they must be accounted for in the design of these units. It was noted in Reference [1] that reducing the concrete modulus has a larger effect on deflection than on stress calculations. This indicates that creep and shrinkage of the concrete affects bridge unit camber more than yield load.

The two most common methods of accounting for creep and shrinkage effects are Branson's method and the reduced modulus method. In Branson's method, actual stress reductions in the concrete due to creep and shrinkage are estimated from empirical formulas. These reductions in concrete stress are used to calculate a more realistic stress distribution in the section, which is then used to calculate a reduced yield load for the unit.

The reduced modulus method is prescribed by the AASHTO Specification [3]. In this method, stresses and deflections due to transient loads such as live load are calculated using the standard transformed section. Stresses and deflections due to sustained loads such as dead load are calculated using a transformed section with the concrete modulus reduced by a factor of 3.0. This amplifies the effects of sustained loads by calculating the resulting stresses and deflections as if they were resisted by a smaller section.

The bridge unit studied in this project was instrumented so that changes in stresses could be measured during construction and testing. In addition, deflection of the beams was measured so that comparisons could be made with predicted values. This was reported in Appendix K of Reference [1] and is repeated here. The three load conditions which the bridge unit was subjected to during construction and testing, along with midspan moment and deflection equations are given in Table B.1. Table B.2 gives a summary of the order, type, and magnitude of the loads resisted by the unit during construction and testing. The first column is an end view of the unit which indicates whether the unit was inverted ($\perp\perp$) or upright ($\top\top$). The "Resisting Section" indicates what portion of the section is assumed to resist the load at that time. It is the steel beams before the concrete had cured and the composite section afterward. The "Loading Type" indicates the distribution of load for that step, corresponding to the load types defined in Table B.1. Measured and predicted stresses for the various stages of construction were listed previously in Table 2.2.

Table B.1

Loading Configurations Used During Construction and Testing of Bridge Units (from Reference 1)

<table>
<tr><th colspan="2">LOADING TYPE</th><th>MIDSPAN MOMENT</th><th>MIDSPAN DEFLECTION</th></tr>
<tr><td>A:</td><td>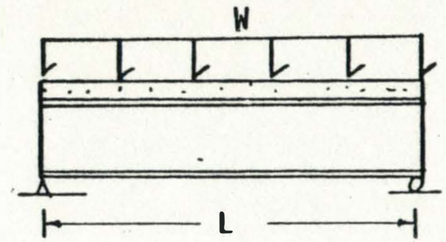
</td><td>$M = \frac{WL^2}{8}$</td><td>$D = \frac{5WL^4}{384\ EI}$</td></tr>
<tr><td>B:</td><td>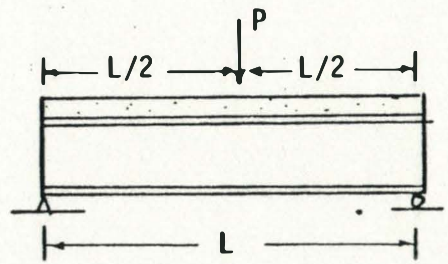
</td><td>$M = \frac{PL}{4}$</td><td>$D = \frac{PL^3}{48\ EI}$</td></tr>
<tr><td>C:</td><td>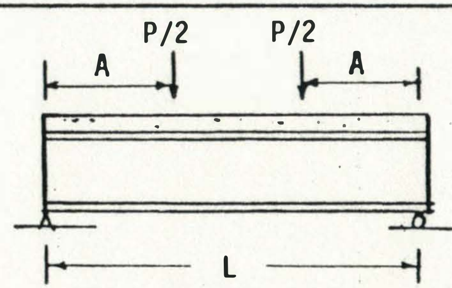
</td><td>$M = \frac{P}{2a}$</td><td>$D = \frac{Pa}{48\ EI}(3L^2-4a^2)$
a = 20'; L = 54'</td></tr>
</table>

Table B.2

Summary of Loading Configurations Used During Construction and Testing of Bridge Units (from Reference 1)

Configuration of Unit	Resisting Section	Loading Type (from Table K.1)	Load Magnitude Unit 1	Load Magnitude Unit 2	Comment
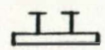	steel beams	A	$W = 0.10^{k/'}$	$0.10^{k/'}$	Steel beams set in inverse position
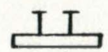	steel beams	A	$W = 0.849^{k/'}$	$0.814^{k/'}$	Steel beams supporting forms and concrete
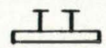	steel beams	B	$P = 3.6^{k}$	8.7^{k}	extra load applied to obtain 3.5" total mid-span deflection
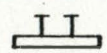	composite unit	B	$P = 3.6^{k}$	8.7^{k}	extra load removed after concrete slab has cured
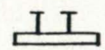	composite unit	A	$W = 0.22^{k/'}$	$0.22^{k/'}$	forms removed
	composite unit	A	$W = 0.729^{k/'}$	$0.694^{k/'}$	unit turned 90°
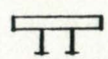	composite unit	A	$W = 0.729^{k/'}$	$0.694^{k/'}$	unit turned additional 90° to upright position
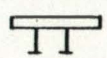	composite unit	A	$W = \pm 0.272^{k/'}$	----	concrete blocks put on and then removed after sustained loading
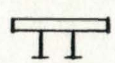	composite unit	C	$P = 7.0^{k}$ Spreader Beam Weight Plus Test Load		test load applied; see App. E for load magnitudes

APPENDIX C

EXAMPLE DESIGN CALCULATIONS

APPENDIX C

This appendix includes sample design calculations for the test bridge unit using both the service load and strength design methods. All calculations use nominal design section and material properties. These calculations are limited to flexure of a single unit and do not consider interaction between units placed side by side to form a complete bridge. Other calculations such as those for shear connector design and web shear checks are the same as for conventional composite girders and are not included in this appendix. Bridge unit dimensions are the same as those in Figure 1.1. Material properties assumed are: concrete $f'_c = 5000$ psi, structural steel $F_y = 50$ ksi, reinforcing steel $F_y = 60$ ksi.

C.1 Service Load Design Method

1. Moments due to various loads:

   Self-weight of steel girders, w = 0.10 klf

   $$M = 0.10\,(54)^2 / 8 = 36.5 \text{ kip-ft}$$

   Self-weight of concrete slab, w = 0.594 klf

   $$M = 0.594\,(54)^2 / 8 = 216.5 \text{ kip-ft}$$

   Weight of concrete formwork, w = 0.22 klf

   $$M = 0.22\,(54)^2 / 8 = 80.2 \text{ kip-ft}$$

   8.7 kip concentrated load at midspan, P = 8.7 kips

   $$M = 8.7\,(54) / 4 = 117.5 \text{ kip-ft}$$

2. Moments applied to inverted bare girders due to:

Steel girder weight	-36.5
Concrete slab weight	-216.5
Concrete formwork	-80.2
8.7 kip concentrated load	-117.5
Total resisted by inverted bare girders =	-450.7 kip-ft

3. Calculate section properties using the standard modular ratio (n = 7) and the increased modular ratio (n = 21) (see Figures C.1 and C.2 respectively).

Concrete Properties
F'c = 5 ksi
n = 7

Reinforcing Steel
Fy = 60 ksi

Beam Steel
Fy = 50 ksi
Area = 14.7 in^2
Sx = 94.5 in^3
Ix = 984 in^4
Number = 2 girders

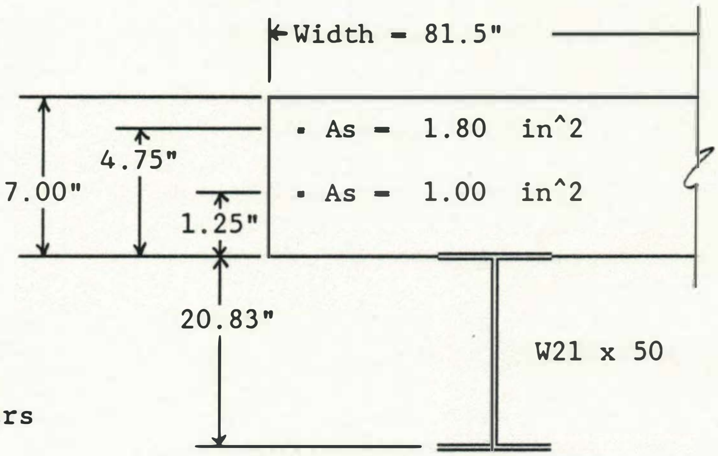

I(base) = 55161.14 in^4
Ybar = 20.72"
I (cg) = 6523.01 in^4

S(top of slab) = 917.34 in^3	S*n =	6421.39 in^3
S(bot of slab) = 58884.31 in^3	S*n =	412190.2 in^3
S(bot of beam) = 314.83 in^3		

	A	y	Ay	Ay^2	Io
Concrete	81.50	24.33	1982.90	48243.84	332.79
Top Bars	1.54	25.58	39.47	1009.55	
Bot Bars	.86	22.08	18.93	417.88	
Stl Beam	29.40	10.42	306.20	3189.08	1968.00
Total	113.30		2347.49	52860.35	2300.79

Figure C.1 Composite Section Properties, n = 7

Concrete Properties
F'c = 5 ksi
n = 21

Reinforcing Steel
Fy = 60 ksi

Beam Steel
Fy = 50 ksi
Area = 14.7 in^2
Sx = 94.5 in^3
Ix = 984 in^4
Number = 2 girders

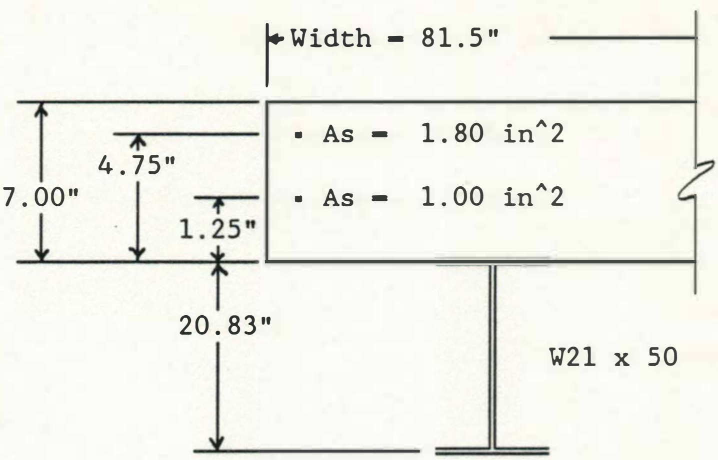

I(base) = 22935.32 in^4
Ybar = 17.42"
I (cg) = 4953.57 in^4

S(top of slab) =	476.00 in^3	S*n =	9996.06 in^3
S(bot of slab) =	1454.11 in^3	S*n =	30536.32 in^3
S(bot of beam) =	284.31 in^3		

	A	y	Ay	Ay^2	Io
Concrete	27.17	24.33	660.97	16081.28	110.93
Top Bars	1.71	25.58	43.85	1121.72	
Bot Bars	.95	22.08	21.03	464.31	
Stl Beam	29.40	10.42	306.20	3189.08	1968.00
Total	59.23		1032.05	20856.39	2078.93

Figure C.2 Composite Section Properties, n = 21

4. Stresses in bare beams due to -450.7 kip-ft moment (while unit is inverted):

$\sigma = M/S = (450.7*12)/(2*94.5) = 28.6$ ksi (T on top, C on bottom)

5. Moments applied to composite section due to:

Remove 8.7 kip concentrated load	+117.5
Remove formwork	+ 80.2
Turn unit 90° (steel beam wt)	+ 36.5
(concrete wt)	+216.5
Turn unit another 90° (steel beam wt)	+ 36.5
(concrete wt)	+216.5
Additional long-term moments resisted by composite section	+703.7 kip-ft

6. Additional stresses in the unit due to the long-term moments: Note that n = 21 section properties are used.

$\sigma_{\text{conc. top of slab}} = (703.7*12)/9996 = 0.845$ ksi (C)

$\sigma_{\text{conc. bot of slab}} = (703.7*12)/30536 = 0.277$ ksi (C)

$\sigma_{\text{steel top of beam}} = (703.7*12)/1454 = 5.81$ ksi (C)

$\sigma_{\text{steel bot of beam}} = (703.7*12)/284.3 = 29.7$ ksi (T)

7. Superimpose stresses from 4 and 6:

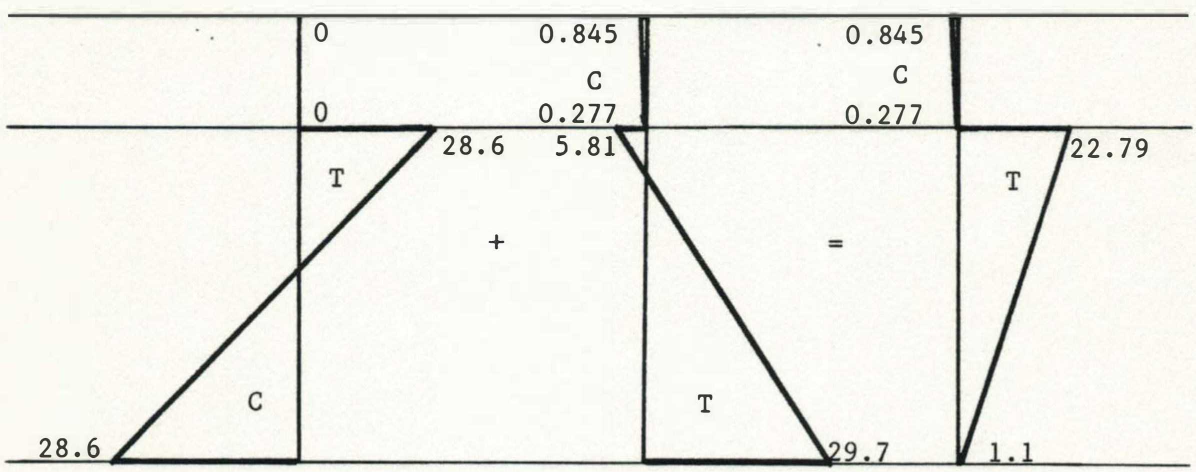

8. Live + impact load moment which will result in beam allowable tensile stress of $0.55F_y = 27.0$ ksi: Note, use regular modular ratio (n = 7) for live load stresses.

$\sigma_{\text{steel bot of beam}} = 27.0 - 1.1 = 25.9$ ksi (T)

M = (25.9*314.8)/12 = 679 kip-ft

(Note, this is the same stress level as for inventory rating)

9. Live + impact moment (for operating rating calculation) which will result in beam tensile stress of $0.75F_y = 37.5$ ksi: Note, use regular modular ratio ($n = 7$) for live load stresses.

$\sigma_{steel\ bot\ of\ beam} = 37.5 - 1.1 = 36.4$ ksi (T)

$M = (36.4*314.8)/12 = 955$ kip-ft

C.2 Strength Design Method

C.2.1 Ultimate flexural capacity

1. Check for compactness of top flange:

   The top flange of the unit is not in compression under noncomposite dead load (AASHTO 10.50(c)) due to the prestressing. In fact, the top flange never experiences compression. Thus it is not necessary for the steel beams to be "compact" in order for the section to develop its plastic moment capacity.

2. Compressive force:

   Slab

   $C = 0.85f'_c bt_s + (AF_y)_c = 0.85(5)(81.5)(7) + 14(.2)(60) = 2593$ kips

   Girders

   $C = AF_y = 2(14.70)(60) = 1470$ kips < 2593 kips

   Therefore, entire depth of girder is in tension.

3. Depth of concrete stress block (neglecting slab steel):

   $a = C\ /(0.85f'_c b) = 1470/346.4 = 4.24$ in

4. Moment capacity (neglecting slab steel):

   $M_u = C \text{ x arm} = C(t_s + d_b/2 - a/2) = 1470\ (7 + 20.83/2 - 4.24/2)$

   $M_u = 22484$ kip-in $= 1874$ kip-ft

   (If slab steel is included, $a = 3.76$ in, $M_u = 1879$ kip-ft)

C.2.2 Examination of operating rating and inventory rating

The operating rating and inventory rating are determined using the procedures outlined in the AASHTO Manual for Maintenance Inspection of Bridges (7). Criteria must be satisfied for both strength and serviceability.

1. Strength requirement: 1.3 [D + RF(L+I)] < maximum strength

   L_o = Operating Rating = (RF)(Rating Moment) = (M_u - 1.3D)/1.3(1 + I)

   Dead Load Moment = $(0.694)(54)^2/8$ = 253.0 kip-ft

   L_o (1 + I) = (1874 - (1.3)(253))/1.3 = 1188 kip-ft

2. Serviceability requirement: [D + RF(L+I)] < serviceability strength

   $L_o = S_{L+I}[0.95F_y - D_1/S_{D1} - D_2/S_{D2}]/(1 + I)$

   From the elastic stress calculations presented previously:

   S_{L+I} = 314.8 in^3

   D_1/S_{D1} = -28.6 ksi (bottom flg. initially put into compression due to prestressing)

   D_2/S_{D2} = +29.7 ksi

   L_o (1 + I) = (314.8) [(0.95)(50) - (-28.6) - (29.7)] = 14607 kip-in

   = 1217 kip-ft > 1188 kip-ft from strength requirement

   Therefore, the operating rating will be governed by the strength requirement, and L_o (1 + I) = 1188 kip-ft.

3. Inventory rating:

   The inventory rating, L_i, is determined as 0.6 times the operating rating.

   L_i (1 + I) = 0.6 (1188) = 713 kip-ft